Animal and human RPC-PET

P.Fonte

FCT
Fundação para a Ciência e a Tecnologia
COMPETE 2020
PORTUGAL 2020
UNIÃO EUROPEIA
Fundo Europeu de Desenvolvimento Regional

Contributors to the RPC-PET project

Current RPC-PET team

Researchers and engineers				Technicians	
Name	**Institute**	**Name**	**Institute**	**Name**	**Institute**
Alberto Blanco	LIP	Michael Traxler	GSI	Americo Pereira	LIP
Antero Abrunhosa	ICNAS	Miguel Couceiro	LIP/ISEC	Carlos Silva	LIP
Custódio Loureiro	FCTUC	Paulo Crespo	LIP	João Silva	LIP
Filomena Clemêncio	ESTSP	Paulo Fonte	LIP/ISEC	Nuno Carolino	LIP
Luís A. V. Lopes	LIP	Rui Alves	LIP		
Miguel C. Branco	ICNAS	Orlando Cunha	LIP		
Nuno Dias	LIP	José Sereno	ICNAS		
Jan Michel	IKF	João Saraiva	LIP		

Past collaborators

Name	Institute	Name	Institute
Adriano Rodrigues	ICNAS/FMUC	Ana Teresa Nunes	LIP
Ângela C.S. Cruz	ICNAS	L. Fazendeiro	LIP
C. Gil	DFUC	Luís Mendes	FMUC
C.M.B.A. Correia	CEI/FCTUC	M. P. Macedo	CEI/FCTUC/ISEC
Carlos Silvestre	ISEC	M.F. Ferreira Marques	FCTUC/ISEC
Durval Costa	HPP	Miguel Oliveira	LIP
Francisco Caramelo	FMUC	Marek Palka	JU
M. Kajetanowicz	NE	Joaquim Oliveira	LIP
Grzegorz Korcyl	JU	Nuno Chichorro	ICNAS/FMUC
Isabel Prata	IBILI	Orlando Oliveira	LIP
J.J. Pedroso Lima	LIP	Paulo Martins	LIP
Jorge André Neves	LIP/FCTUC	Rui F. Marques	LIP/FCTUC
Jorge Landeck	FCTUC	Francisco Oliveira	ICNAS/UC

CEI: Centro de Electrónica e Instrumentação, Univ. Coimbra, Portugal.
ESTSP: Escola Superior de Tecnologia da Saúde do Porto, Portugal
FCTUC: Departamento de Física da Faculdade de Ciências e Tecnologia da Universidade de Coimbra.
FMUC: Faculdade de Medicina da Universidade de Coimbra.
GSI: Helmholtz Centre for Heavy Ion Research, Darmstadt, Germany
HPP: Hospitais Privados do Porto, Porto, Portugal
IBILI: Instituto Biomédico de Investigação da Luz e Imagem da Faculdade de Medicina da Universidade de Coimbra
ICNAS: Instituto de Ciências Nucleares Aplicadas à Saude da Universidade de Coimbra, Coimbra, Portugal.
IKF: Institut für Kernphysik, Goethe-Universität, Frankfurt, Germany
ISEC: Instituto Superior de Engenharia de Coimbra, Coimbra, Portugal.
JU: Jagiellonian University of Cracow, Cracow, Poland.
LIP: Laboratório de Instrumentação e Física Experimental de Partículas, Coimbra, Portugal.
NE: Nowoczesna Elektronika, Crakow, Poland

The basic idea for RPC-based TOF-PET

The converter-plate principle

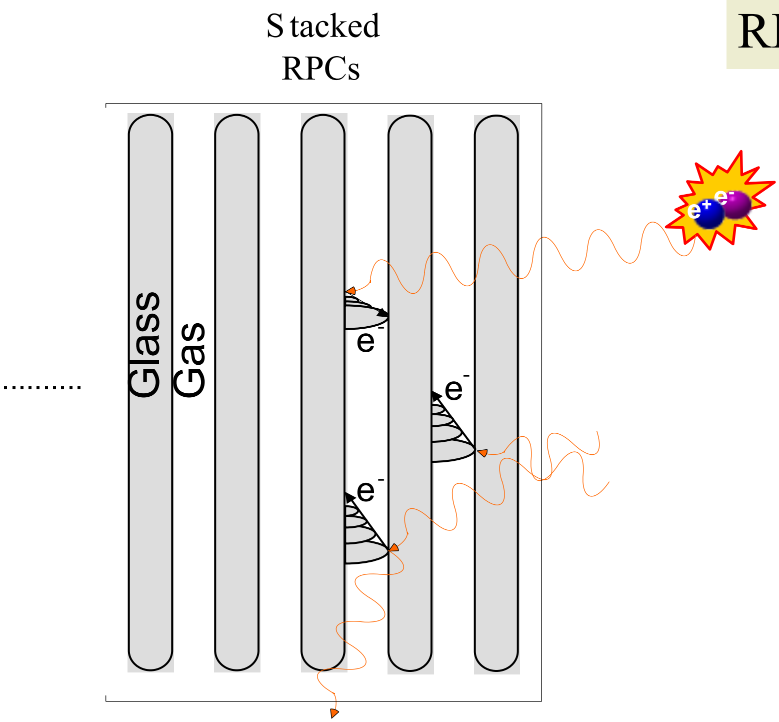

Use the electrode plates as a γ converter, taking advantage of the natural layered construction of the RPCs.

[Blanco 2002]

Time resolution for 511 keV photons:
(our routine lab-test tool)

90 ps σ for 1 photon

300 ps FWHM for the photon pair

A previous work on PET with gaseous detectors (21 lead plates + 20 MWPCs = 7% efficiency)

"The Rutherford Appleton Laboratory's Mark I Multiwire Proportional Counter Positron Camera"
J.E. Bateman et al. NIM 225 (1984) 209-231

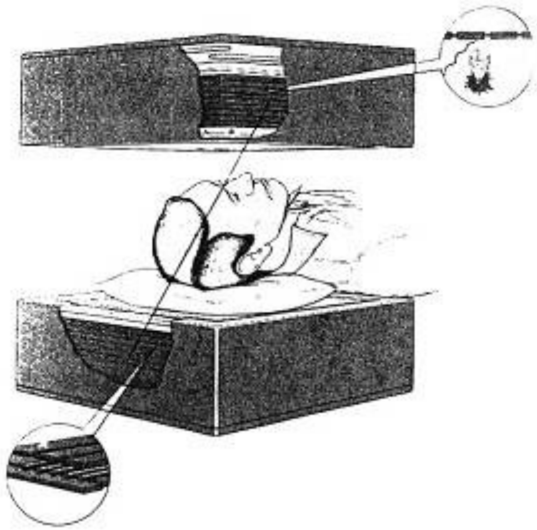

Started a long time ago…

Available online at www.sciencedirect.com

SCIENCE DIRECT®

ELSEVIER

Nuclear Instruments and Methods in Physics Research A 508 (2003) 88–93

NUCLEAR INSTRUMENTS & METHODS IN PHYSICS RESEARCH Section A

www.elsevier.com/locate/nima

Perspectives for positron emission tomography with RPCs☆

A. Blanco[a,b], V. Chepel[a,c], R. Ferreira-Marques[a,c], P. Fonte[a,c,d,*], M.I. Lopes[a,c], V. Peskov[e], A. Policarpo[a,c]

[a] *LIP–Laboratório de Instrumentação e Física Experimental de Partículas, Portugal*
[b] *GENP, Dept. Fisica de Particulas, Univ. Santiago de Compostela, Spain*
[c] *Departamento de Física da Universidade de Coimbra, Coimbra, Portugal*
[d] *Instituto Superior de Engenharia de Coimbra, Coimbra, Portugal*
[e] *Royal Institute of Technology, Stockholm, Sweden*

Excellent position resolution ⇒ small animal PET

Affordable in large areas
⇒ full-body field of view human PET
⇒ promising increased sensitivity at physics-limited resolution

Comparison with the standard PET technology

Disadvantages

Certainly a much smaller efficiency: 20 to 50% as compared to 70 to 80%.
No energy resolution, but there is an equivalent energy sensitivity... more later.
Detector scatter (vs. "misidentified fraction" in crystal blocks)

Possible specialized PET applications

Advantages

Increasing system sensitivity

Inexpensive ⇒ large areas possible ⇒ large solid angle coverage
Excelent timing ⇒ TOF-PET possible+optimum randoms rejection

} Whole-body Human PET

Increasing position accuracy

Gaseous detectors routinely deliver 0.1 mm resolution
Full 3D localization possible ⇒ no gross parallax error
The very small gap minimizes intrinsic errors

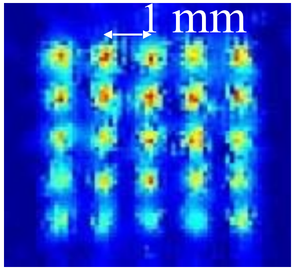

Simulation: 0.51mm FWHM

} Small Animal PET

Other

Simultaneous full body imaging (continuous uptake signal)
Compatible with magnetic field ⇒ PET-MRI can be considered

Comparison with GEANT - efficiency

Optimum efficiency is balanced by beam absorption (thicker plates) and extraction probability (thinner plates)

Optimum thickness depends on the number of plates and on the material.

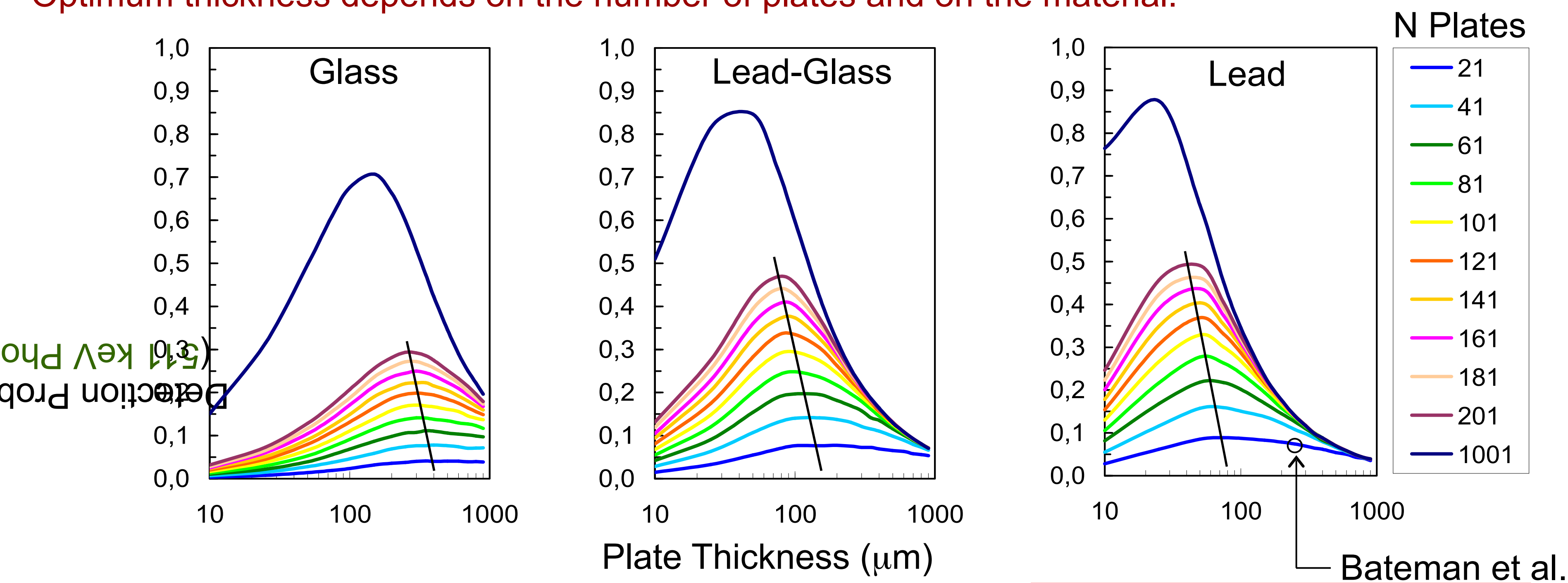

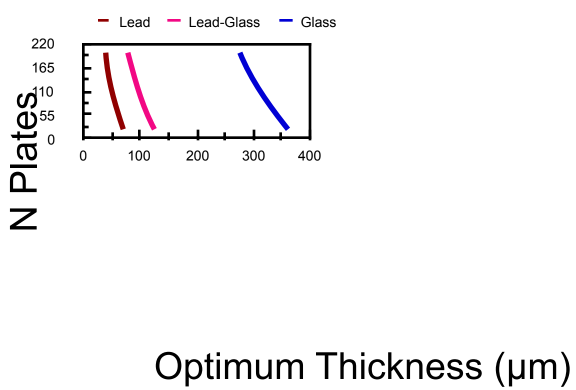

Our measurement:
for few gaps
~0.2%/gap
@ 511 keV

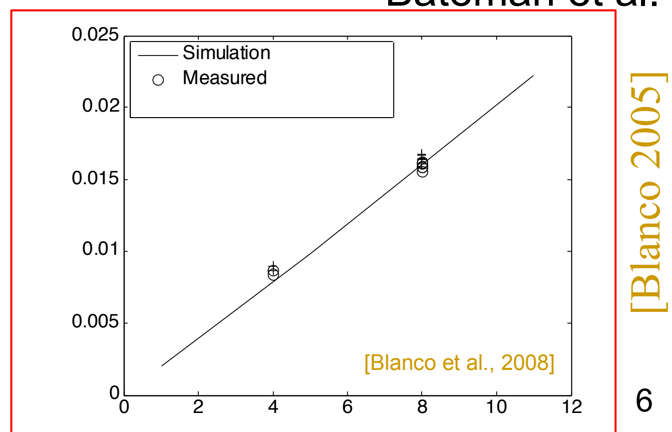

GEANT - energy dependence

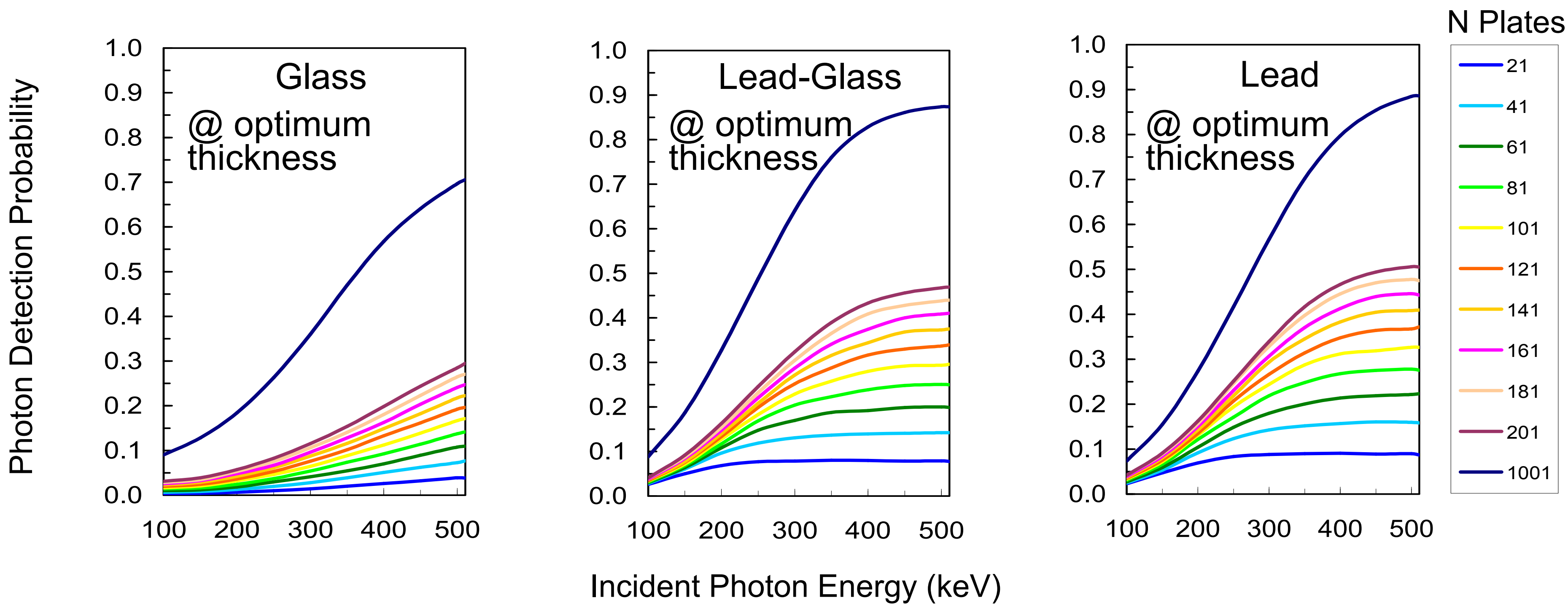

Strong ENERGY SENSITIVY
scattered photons statistically rejected

	ε_{max}	Glass	Lead-Glass	Lead
		Material		
N Plates	101	*17%*	*29%*	*31%*
	201	*29%*	*47%*	*50%*

Intrinsic sources of instrumental position error

The converter-plate principle

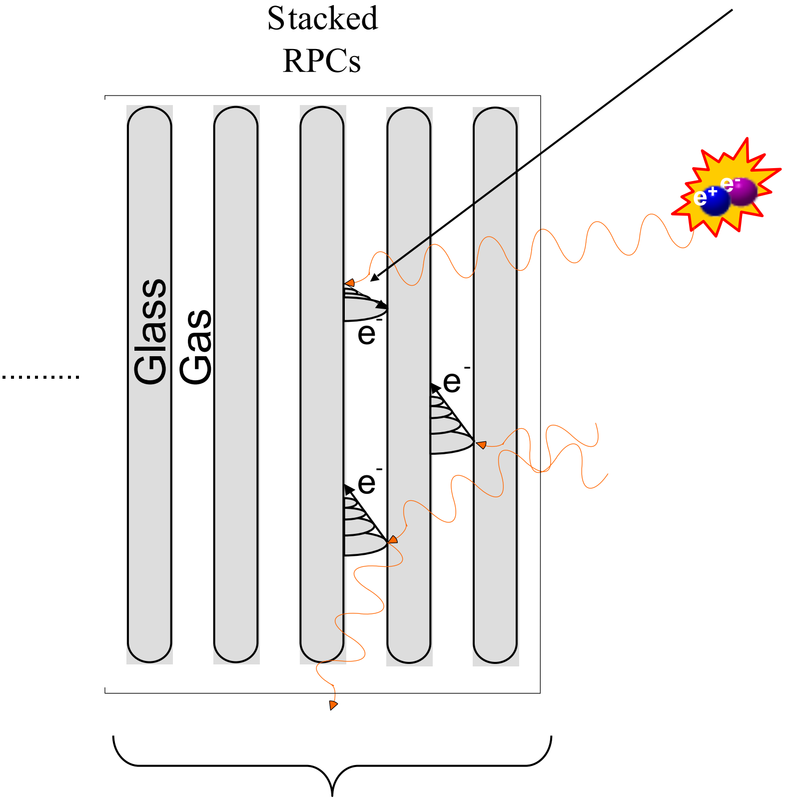

- Electronic noise
- Angle of ejection of the electron will shift the baricenter of the avalanche.

⇒ Minimized by very thin gas gap

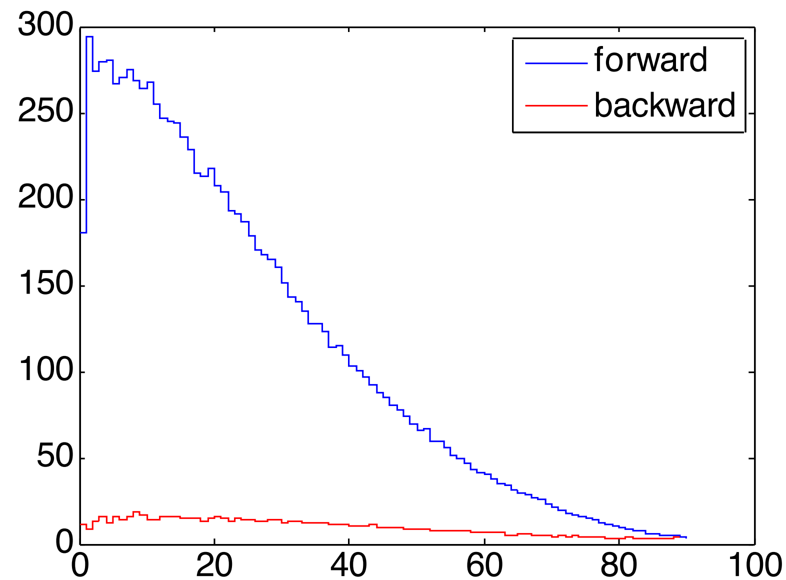

- Different gaps fired along an inclined trajectory cause parallax error (depth of interaction – DOI error)

⇒ Identification of the fired gap by analysis of the induced charge pattern

Small animal PET

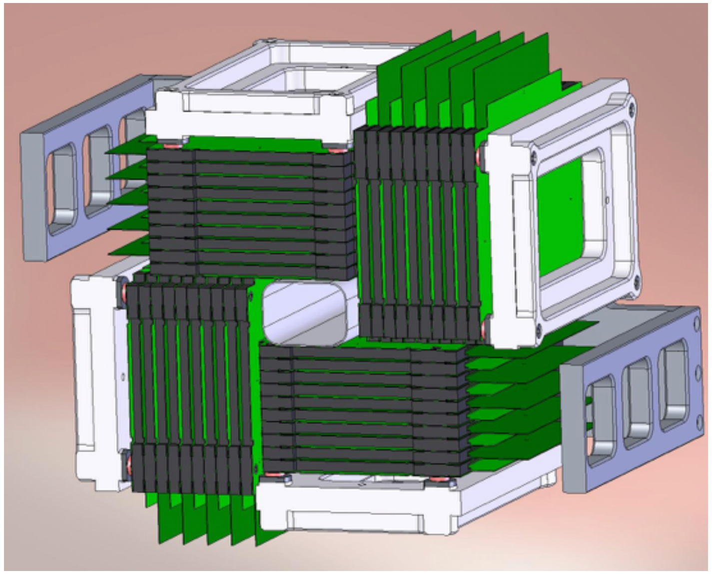

Small animal PET - a first prototype

Charge-sensitive electronics allowing interstrip position interpolation

Aimed at **verifying** the concept and show the **viability** of a **sub-millimetric spatial resolution**.

16 stacked RPCs

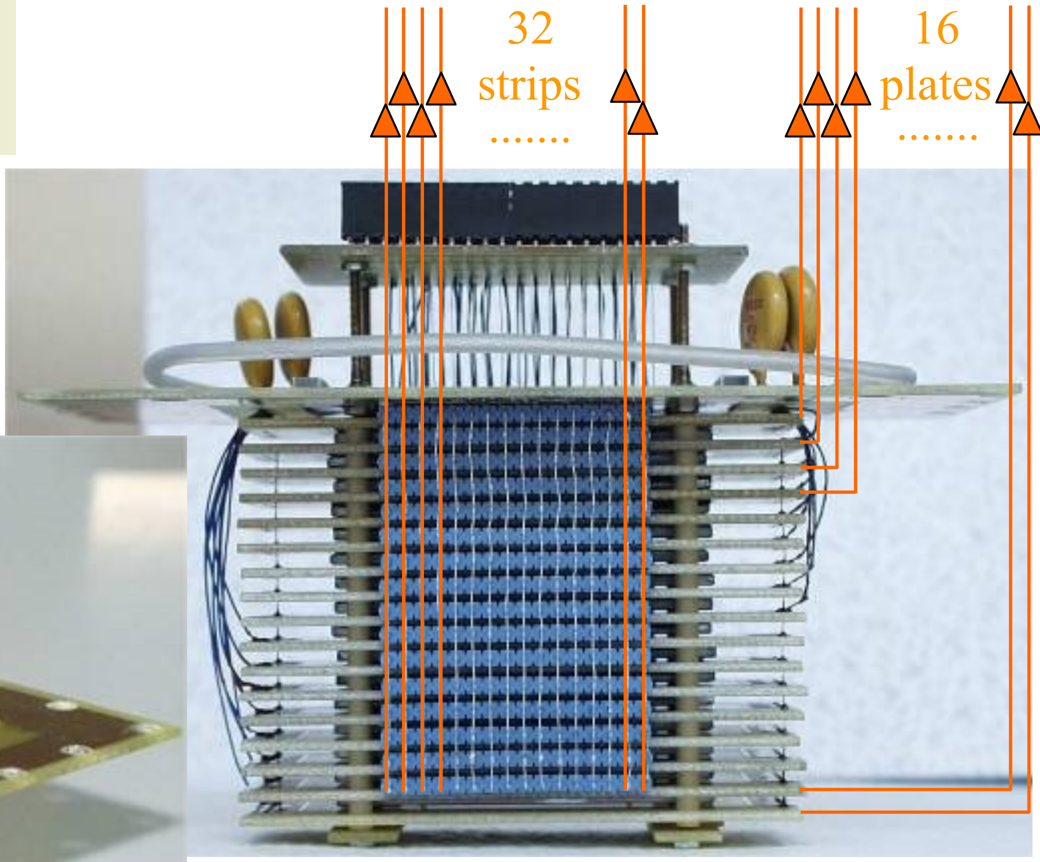

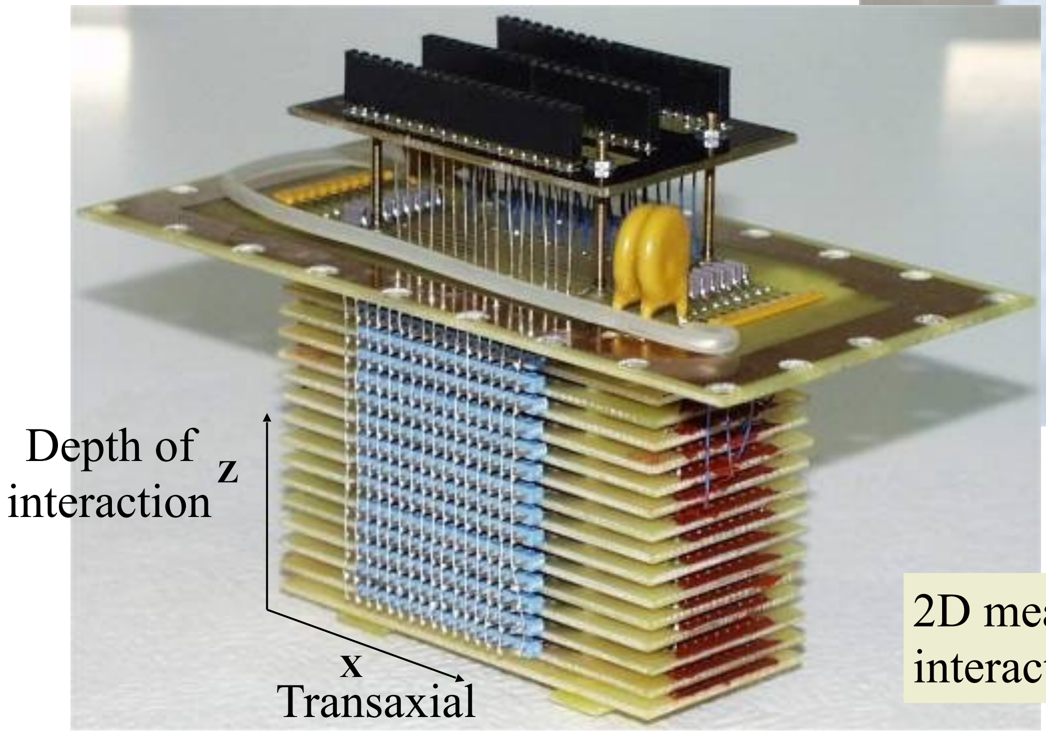

(now enjoying a second life as an exhibition item)

2D measurement of the photon interaction point

System in action

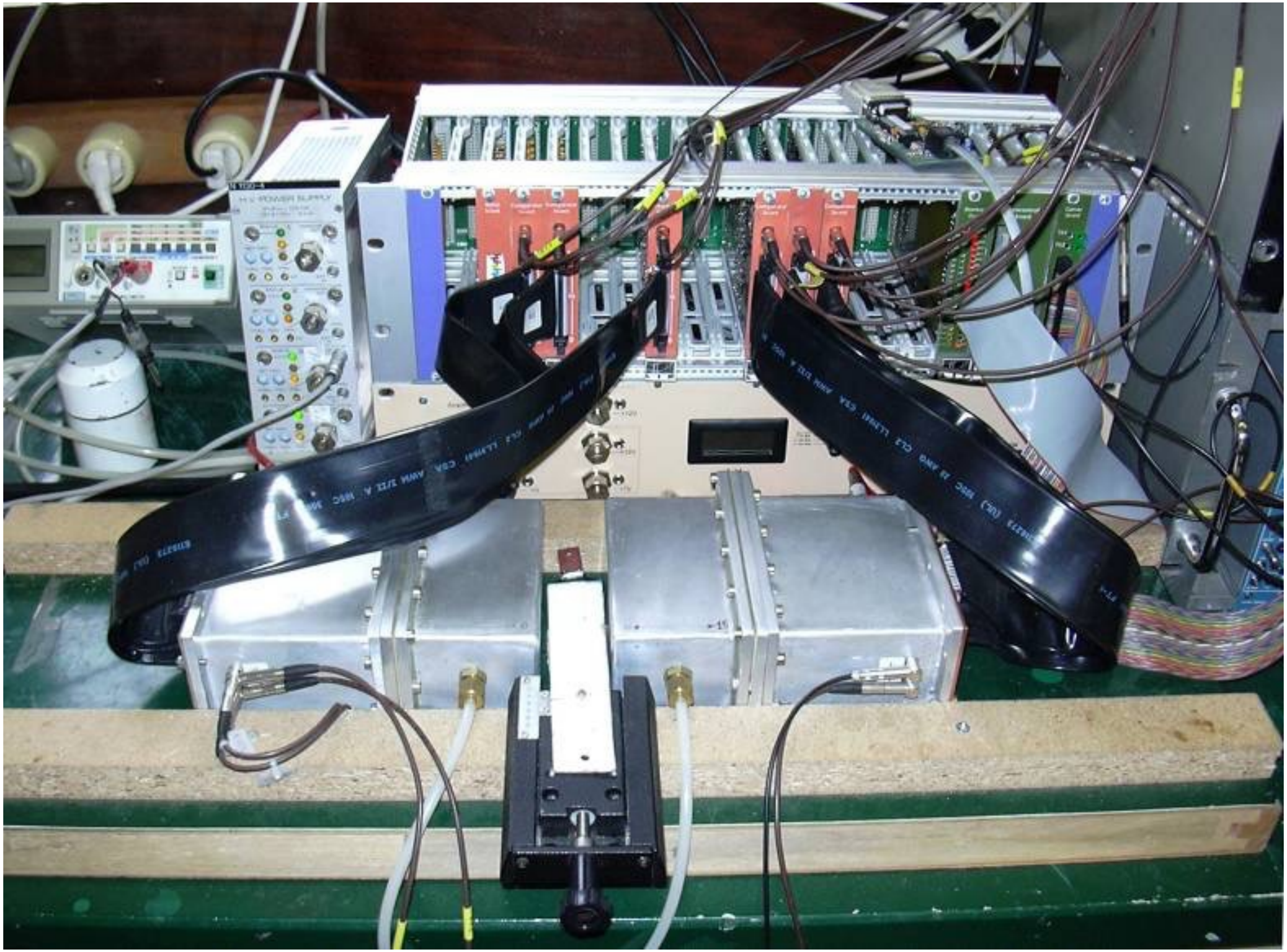

Image spatial resolution (gaussian fitting)

Filtered Back Projection FBP

~ 465 μm FWHM

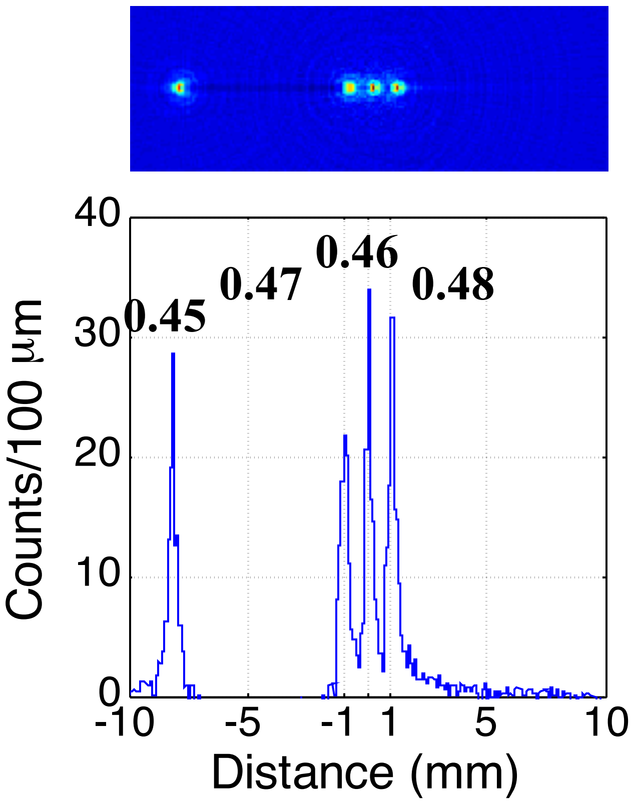

[A.Blanco, IEEE MIC 2004, PhD thesys]

Maximum likelihood-expectation maximization with resolution modeling (ML-EM)

~ 305 μm FWHM

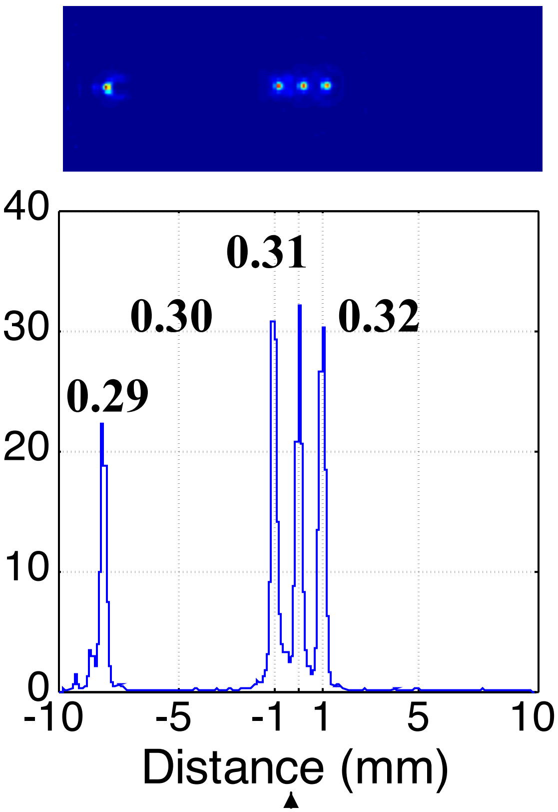

Proceeding IEEE MIC (2004) M2-177

Homogeneous spatial resolution over the entire field of view

Full scanner for mice – project

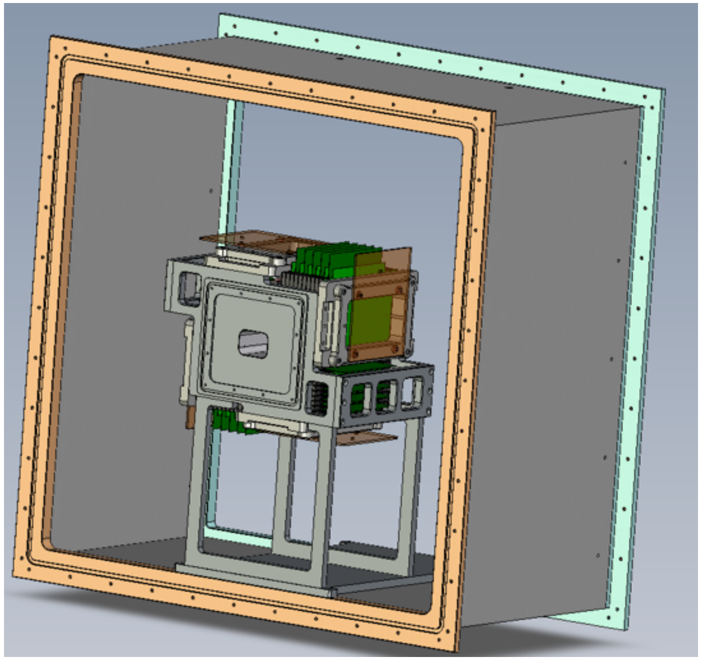

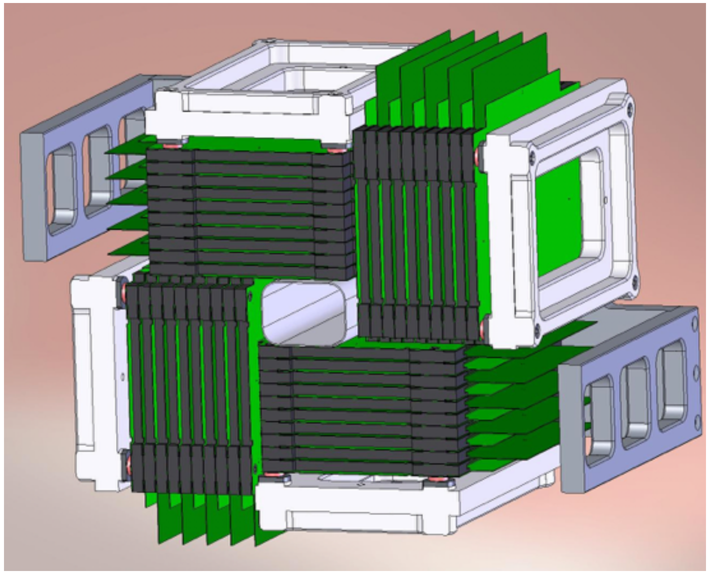

Almost 4π coverage

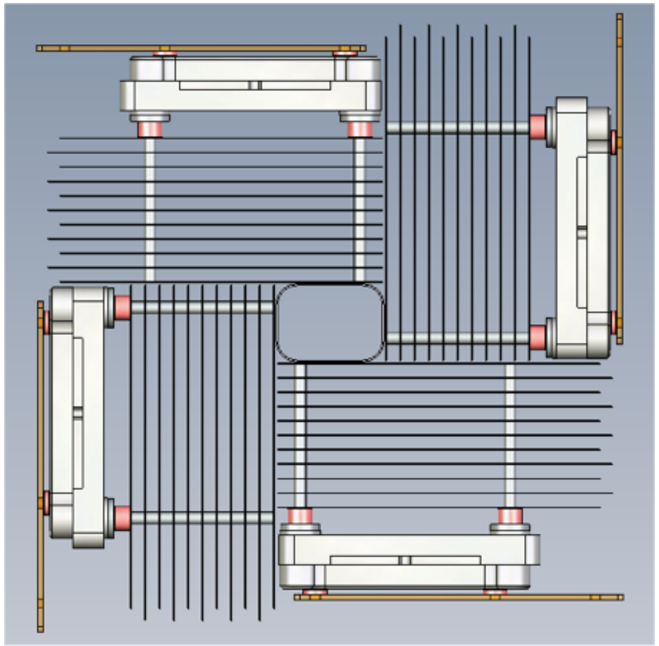

Detector & readout

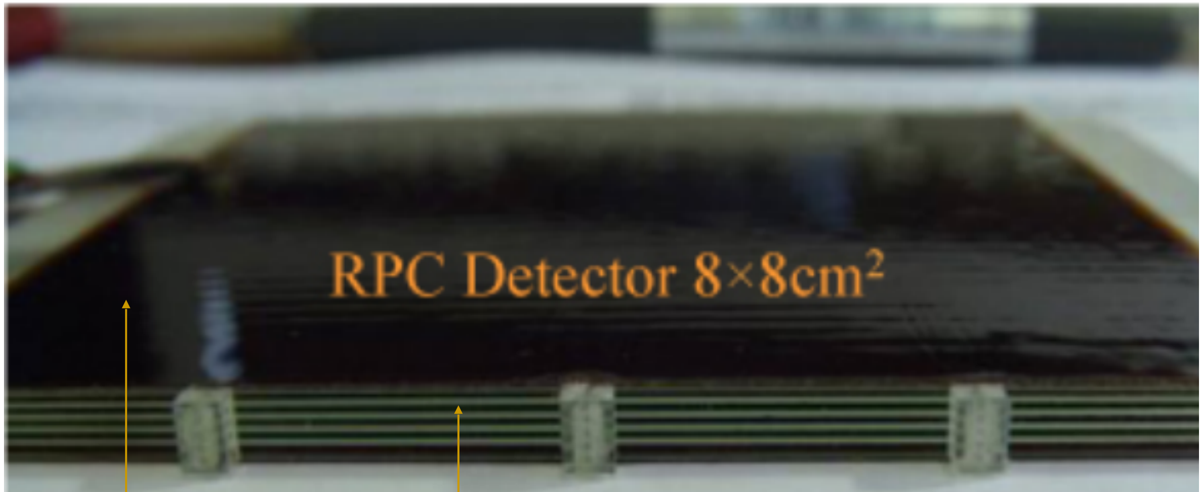

HV distribution layer
(signal-transparent)
kapton insulation

5 gaps 0.35 mm
6 x 0.38mm glass
~5 mm thick

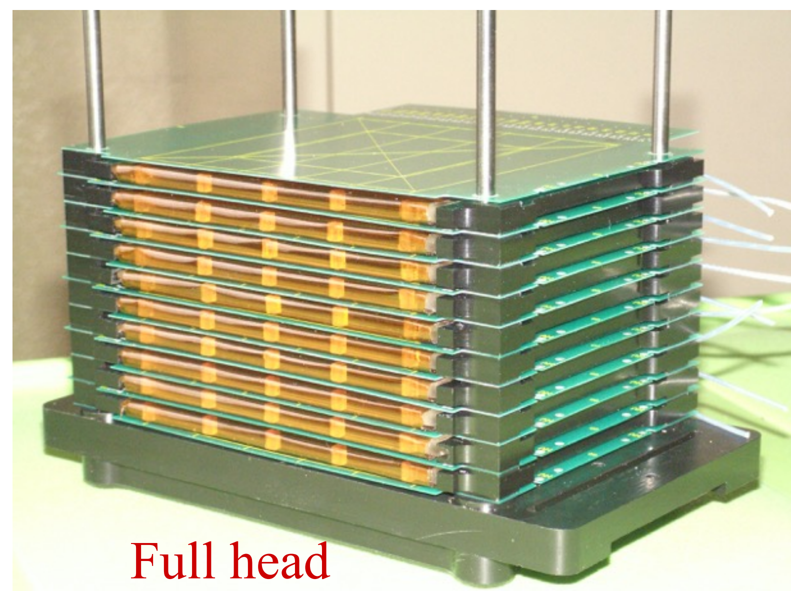

Preliminary resolution tests in simplified geometry but realistic readout

Two detectors with XY localization

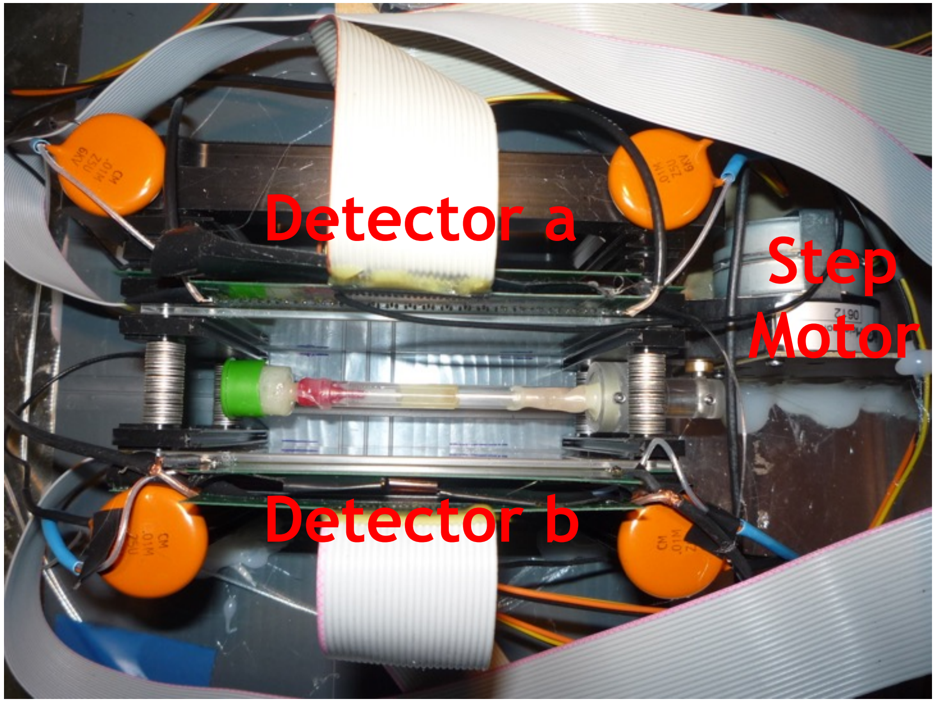

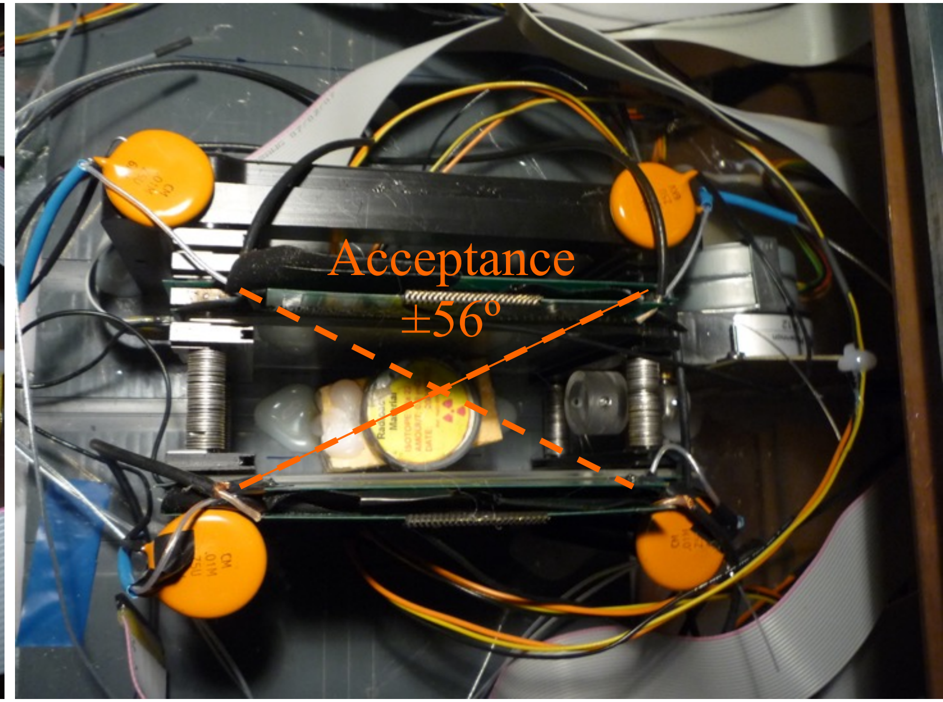

Needle source, 0.2 mm ∅ int.

Planar (disk) source

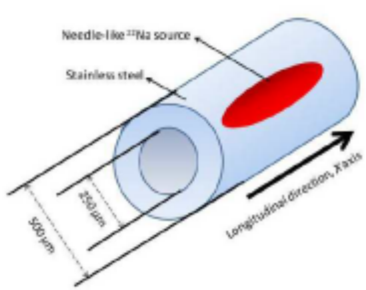

[P.Martins et al., JINST 2014 + PhD thesys]

Preliminary resolution tests in simplified geometry but realistic readout

Full area, all angles (up to 56º),
all gaps (DOI)
MLEM reconstruction
(no resolution modeling)

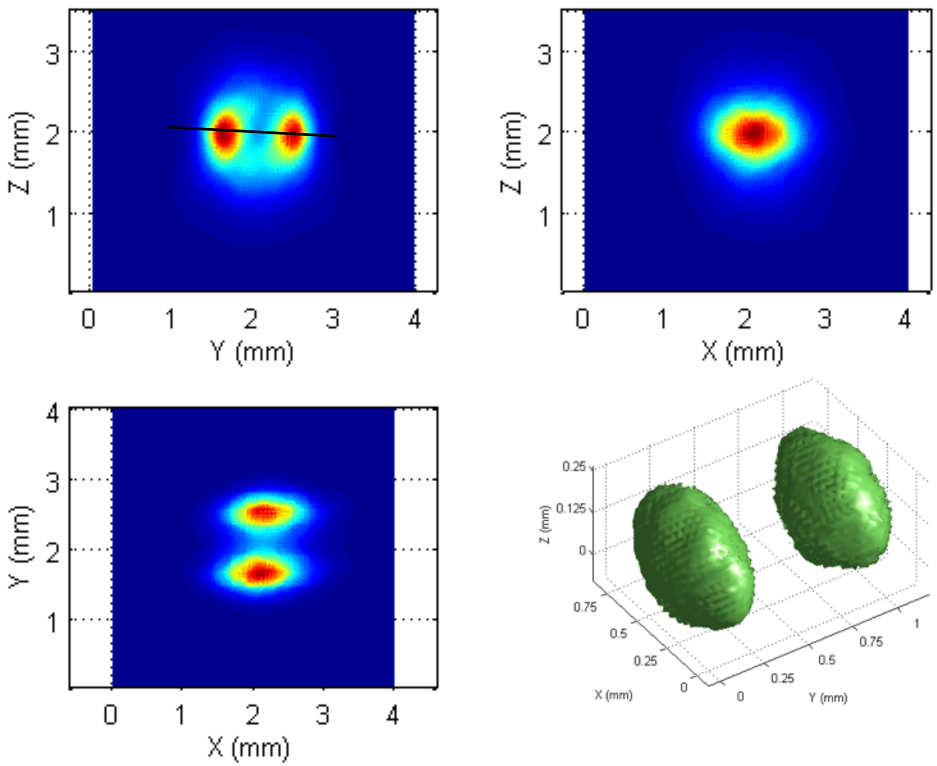

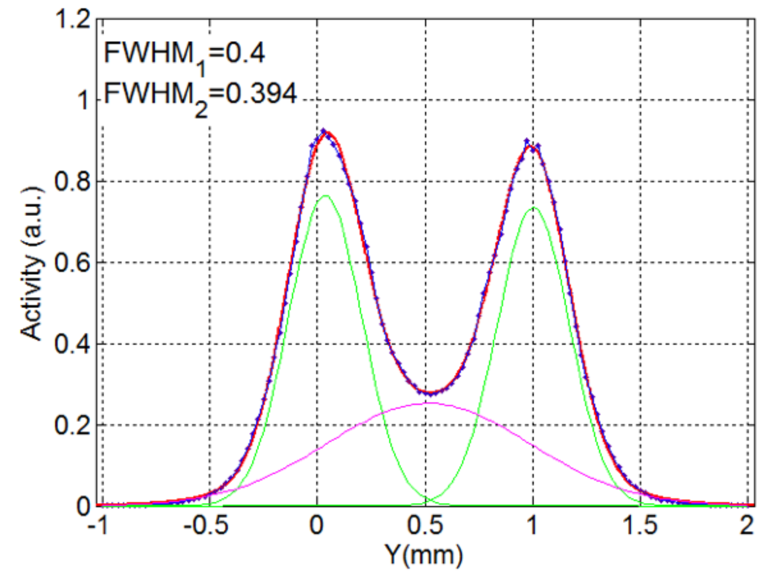

Joint reconstruction of the source in 2 positions separated by 1mm.
~130k LORs in 3.5M 25μm voxels.
Color maps: planar profiles including peak density point.
Isosufaces: 50% rel. activity

Reconstructed activity profile across the black line shown in the upper left panel.
Resolution **~0.4mm FWHM**
+background
(Note: source is 0.2mm diam.)

[P.Martins et al., JINST 2014 + PhD thesys]

Construction at LIP (2013/14)

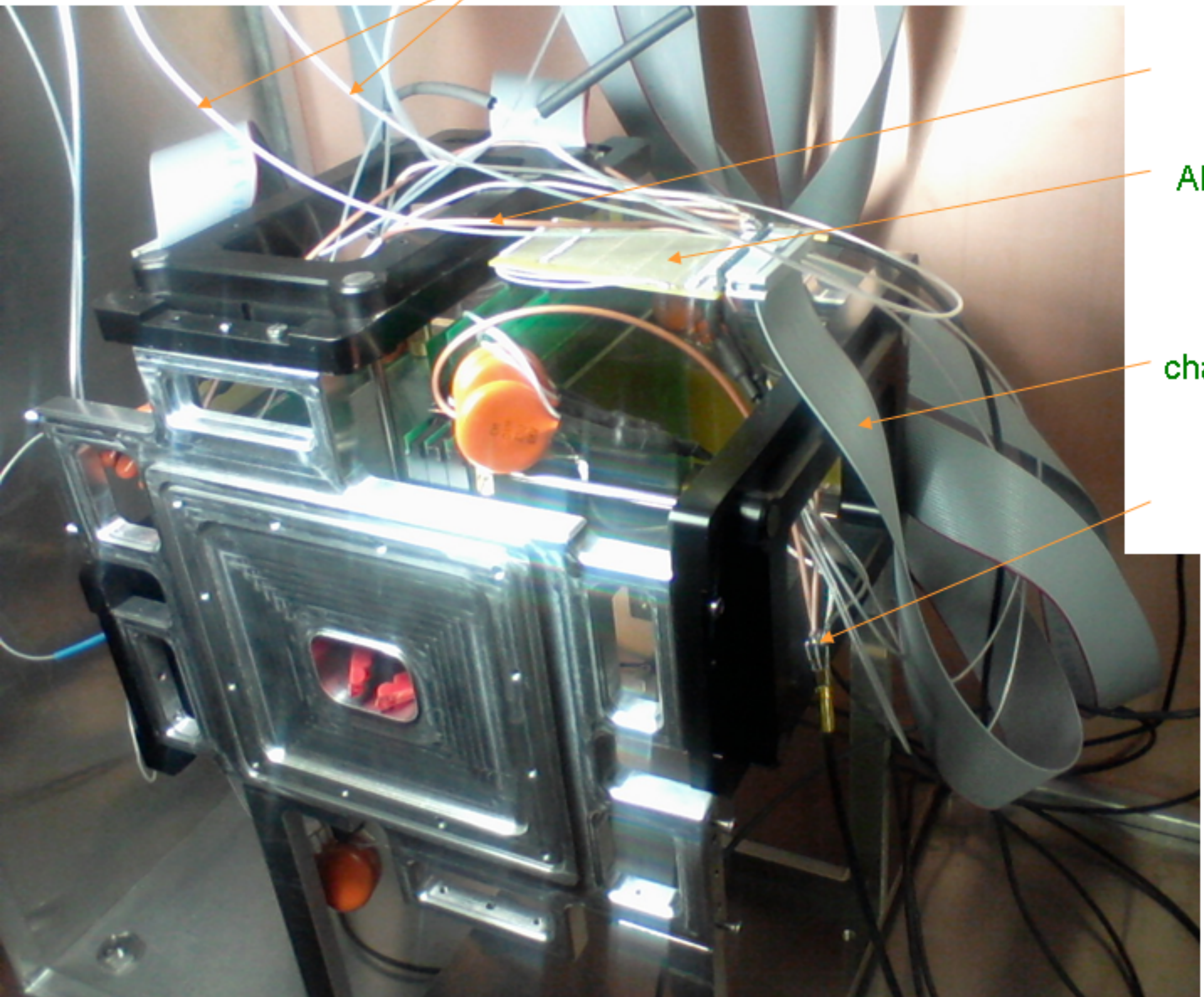

Resolution in final geometry (2 heads only, needle source)

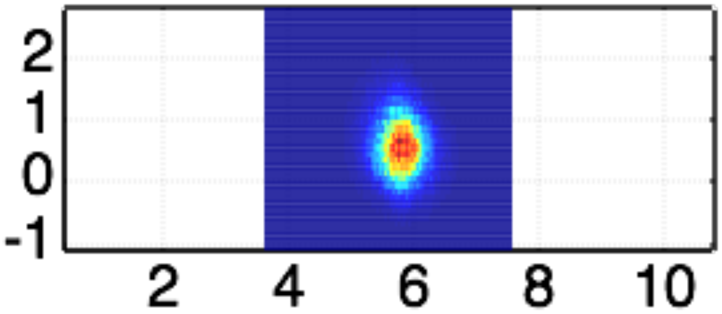

X'

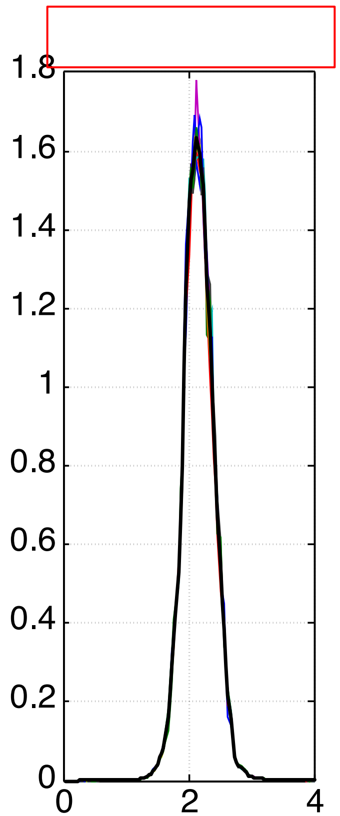

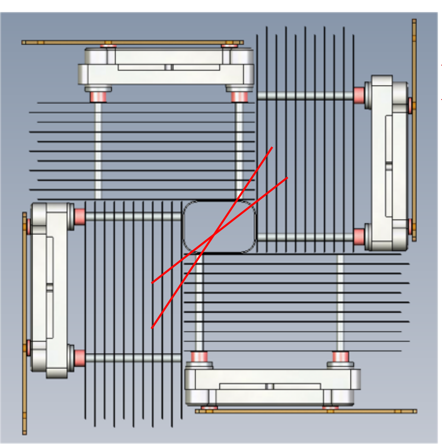

PRELIMINARY
Calibration not done in full.

Installed at ICNAS (UC) in July 2014

Upgrades 2015,17

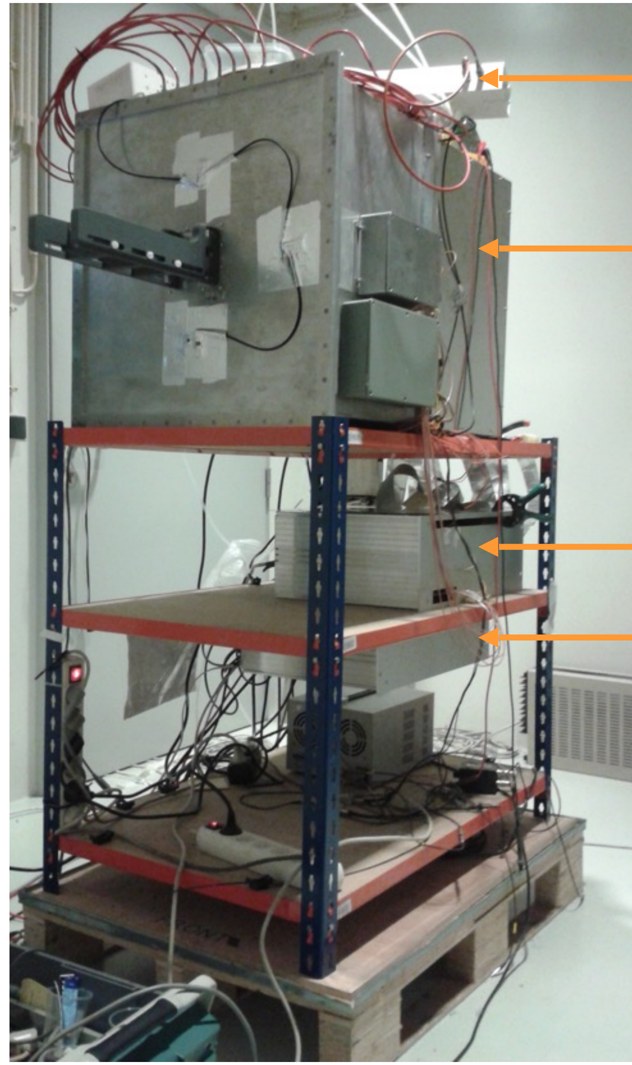

Readout electronics (for both PETs)

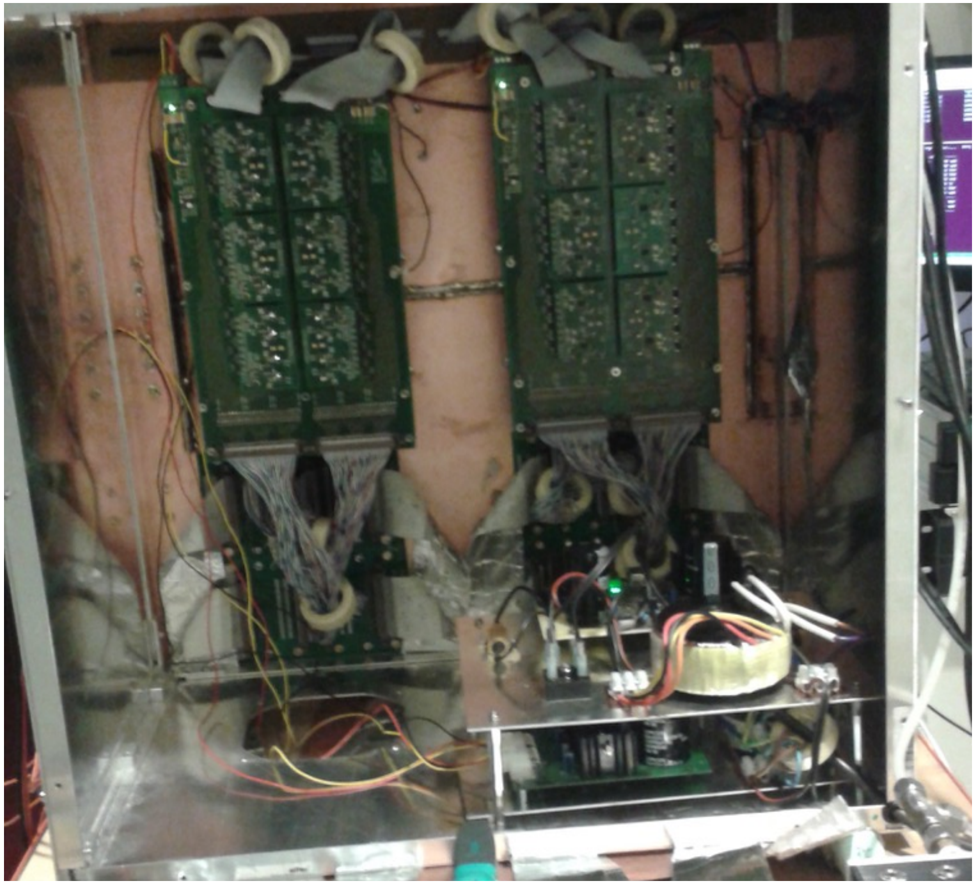

48 channel charge amplifier boards,
optimized for large input capacitance.
Each animal PET head needs one such board
-> 192 channels

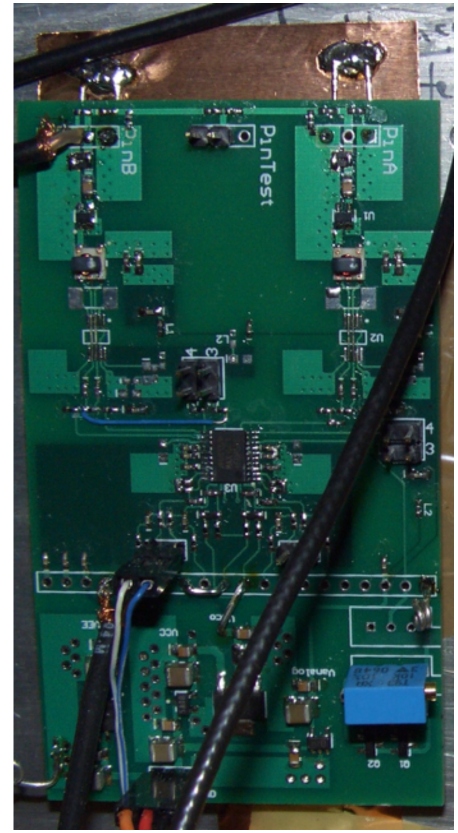

Timing electronics
2 channels @ 3 cm pitch
2 amps + dual discriminator
GHz bandwidth
output: LVDS + analog sum
accuracy ~few tens of ps

Readout electronics (for both PETs)

TRB3 platform developed by the *TRB collaboration* (trb.gsi.de)

Configurable trigger system (C.Loureiro/UC + F.Clemencio/ESTSP)

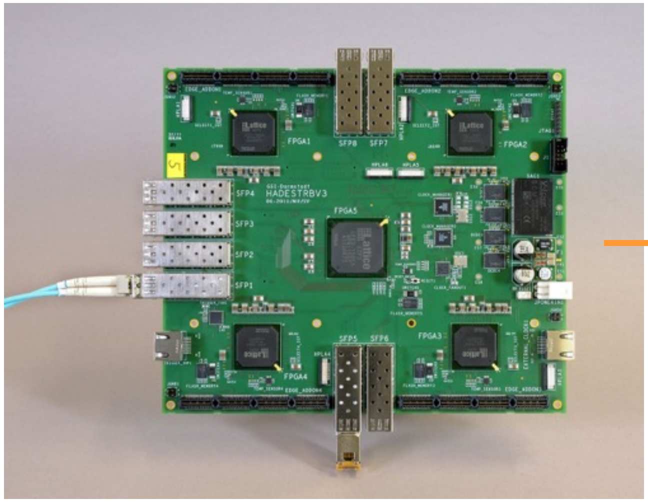

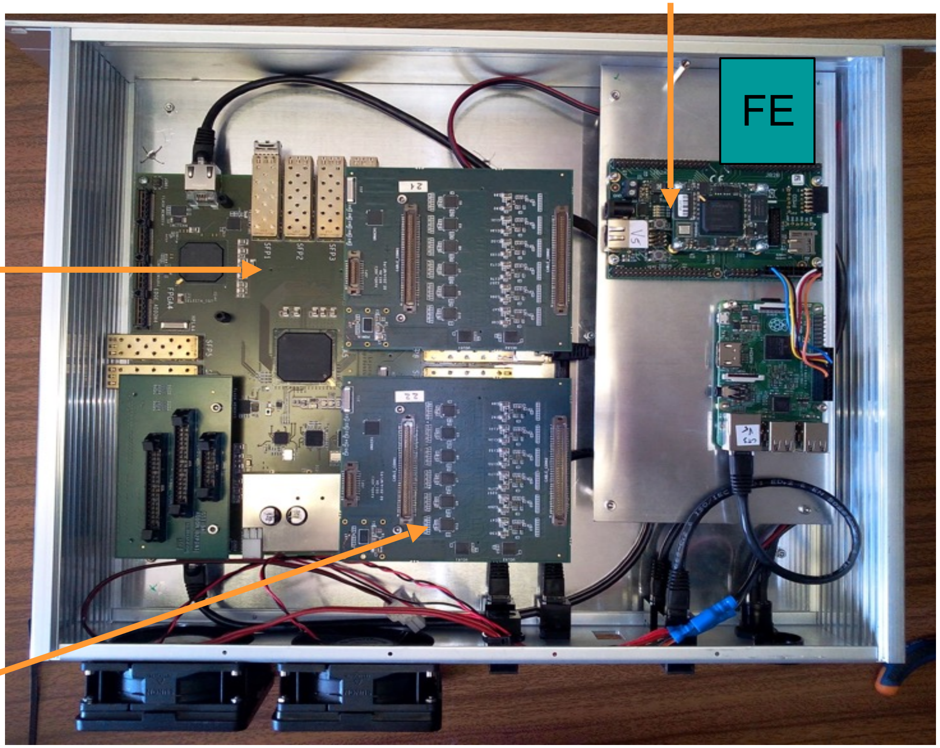

ADCaddon (48 ch @ 40MSPS) (Jan Michel IKF)

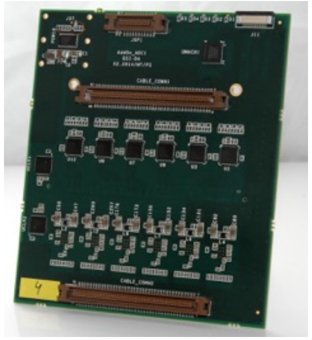

First client (31/7/2014)

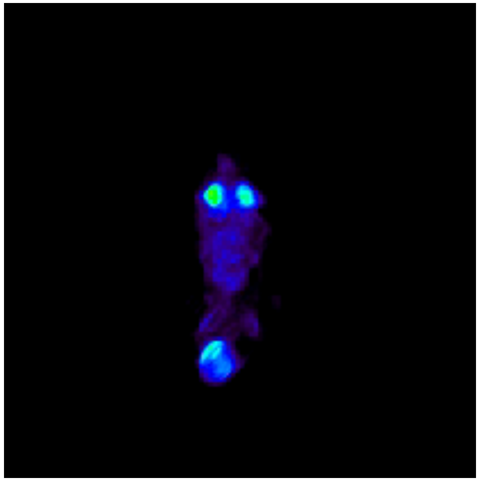

Poor animal resting after **18FDG** injection and in the scanner tunnel
(The head is central and the heart is at the edge of the field-of-view)

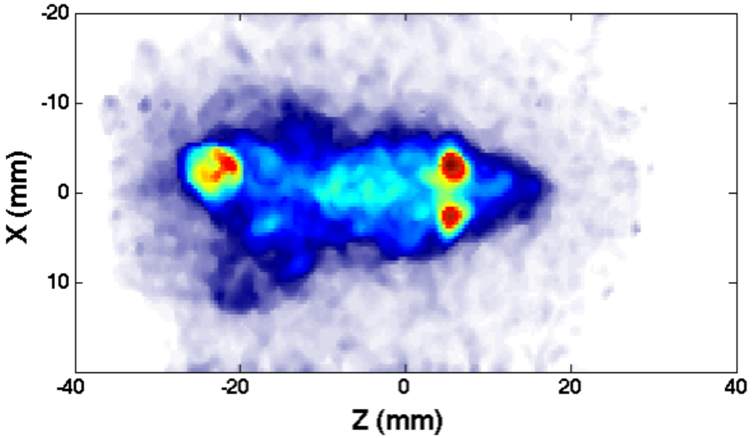

- Maximum intensity projection.
- The two hot spots in the head are likely the Harderian glands and the heart walls seem resolved

Some interesting images of mice

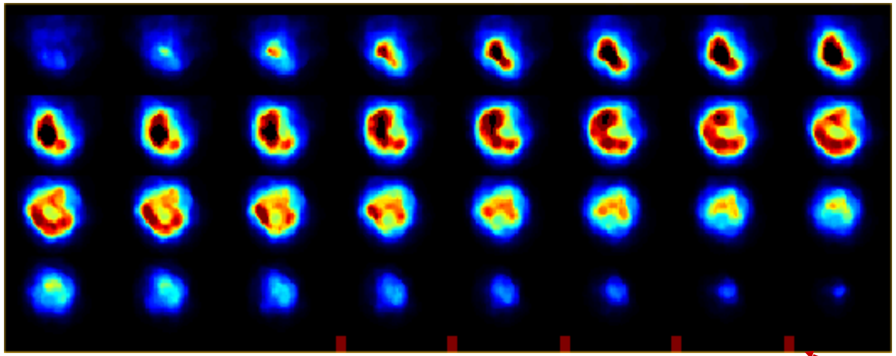

Live heart transaxial sections with ^{18}FDG

1 mm^2

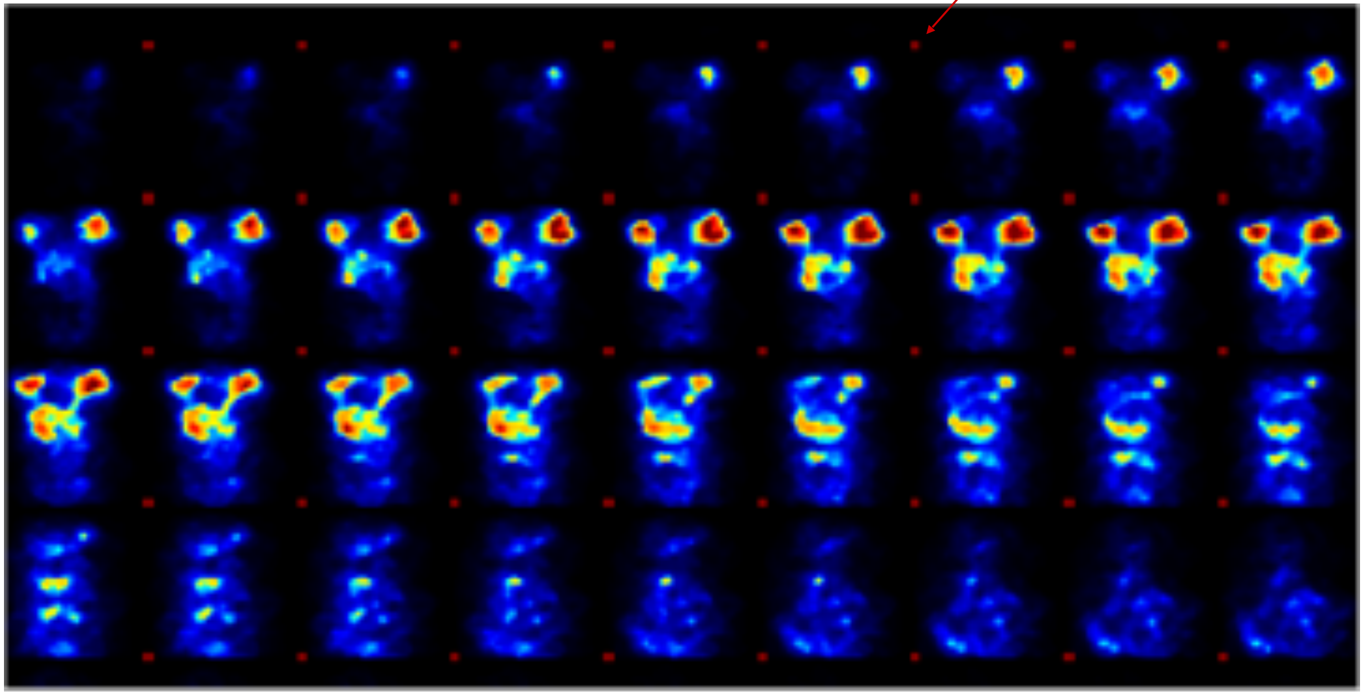

Harderian glands and left striatum with ^{11}C-raclopride

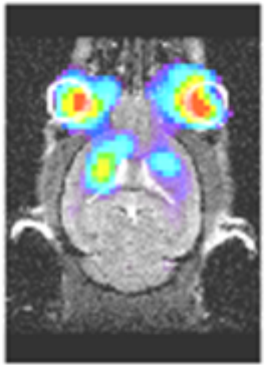

Co-registration with MRI

Some interesting images of mice

11C Raclopride (ratinho I)

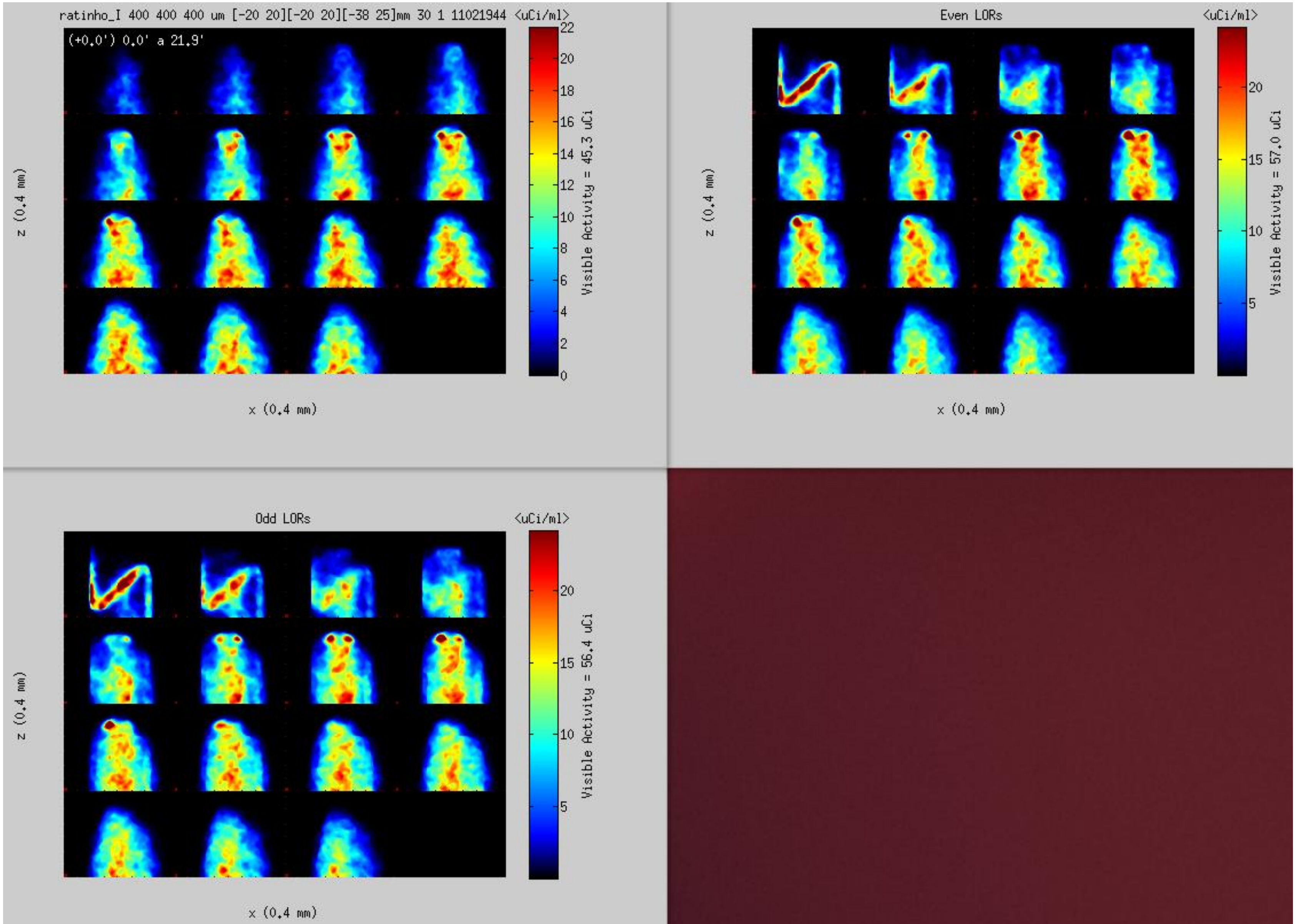

Some interesting images of mice

64Cu ASTM (ratinho G)

Some interesting images of mice

64Cu ASTM (recent)
Co-registration with MRI (Francisco Oliveira, José Sereno)

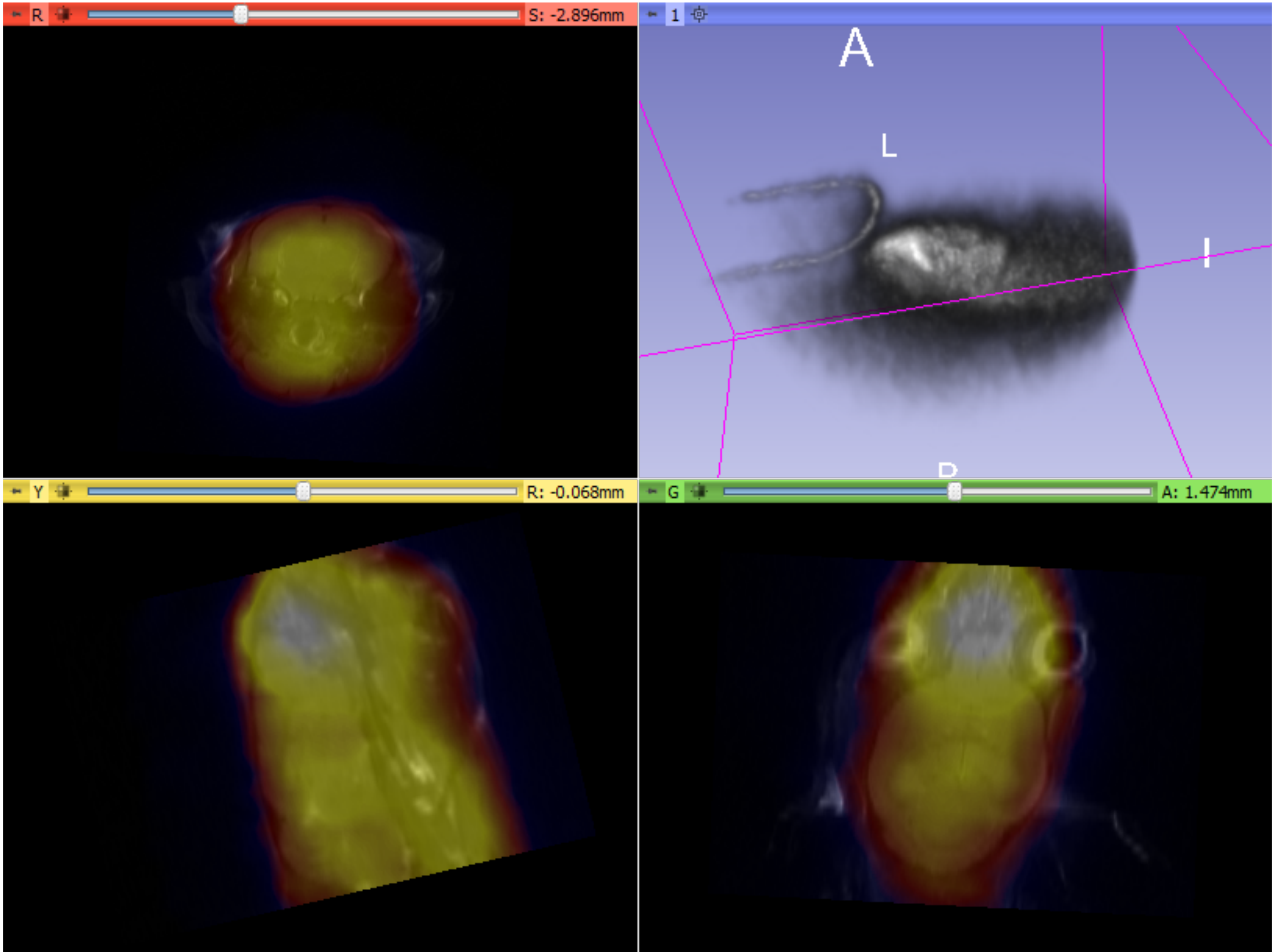

Enlarged for rats (2015)

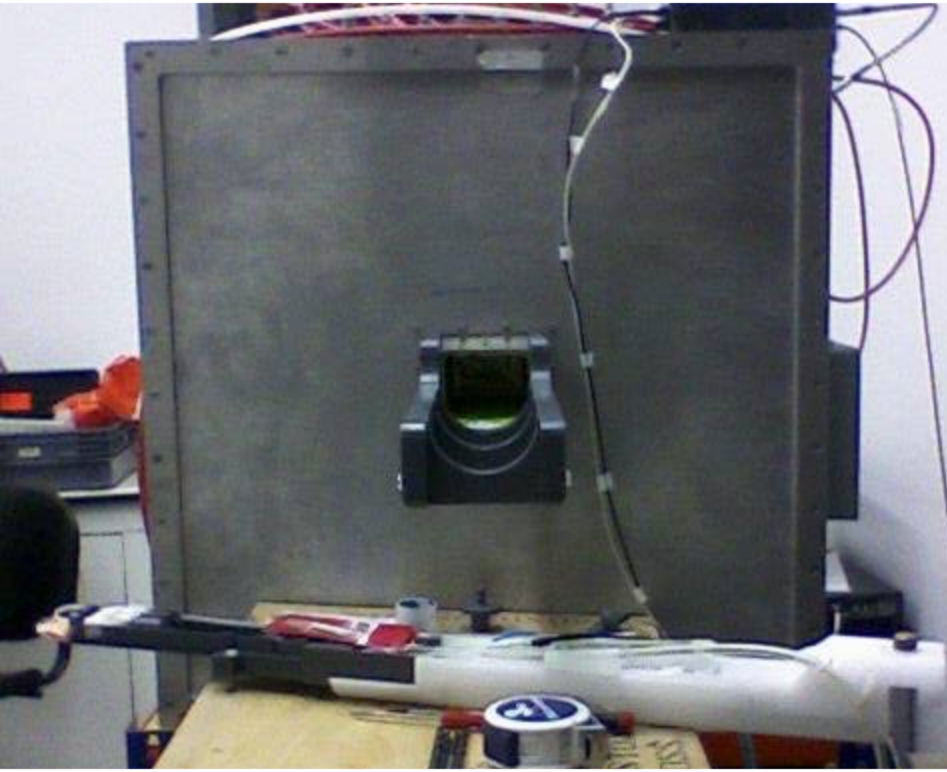

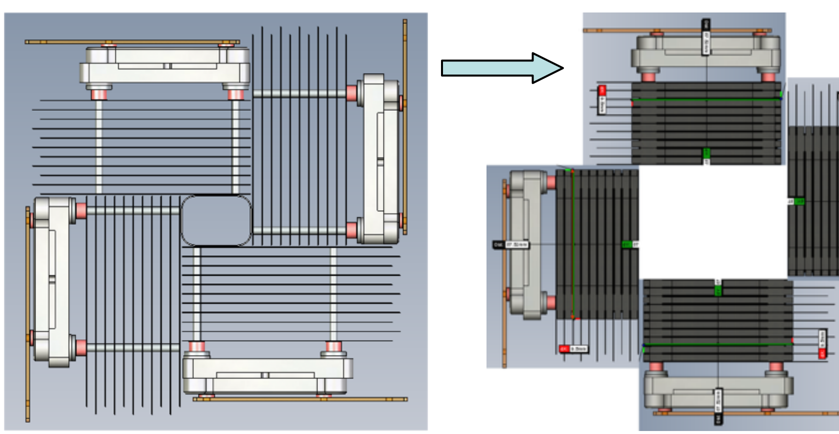

Rats A & B

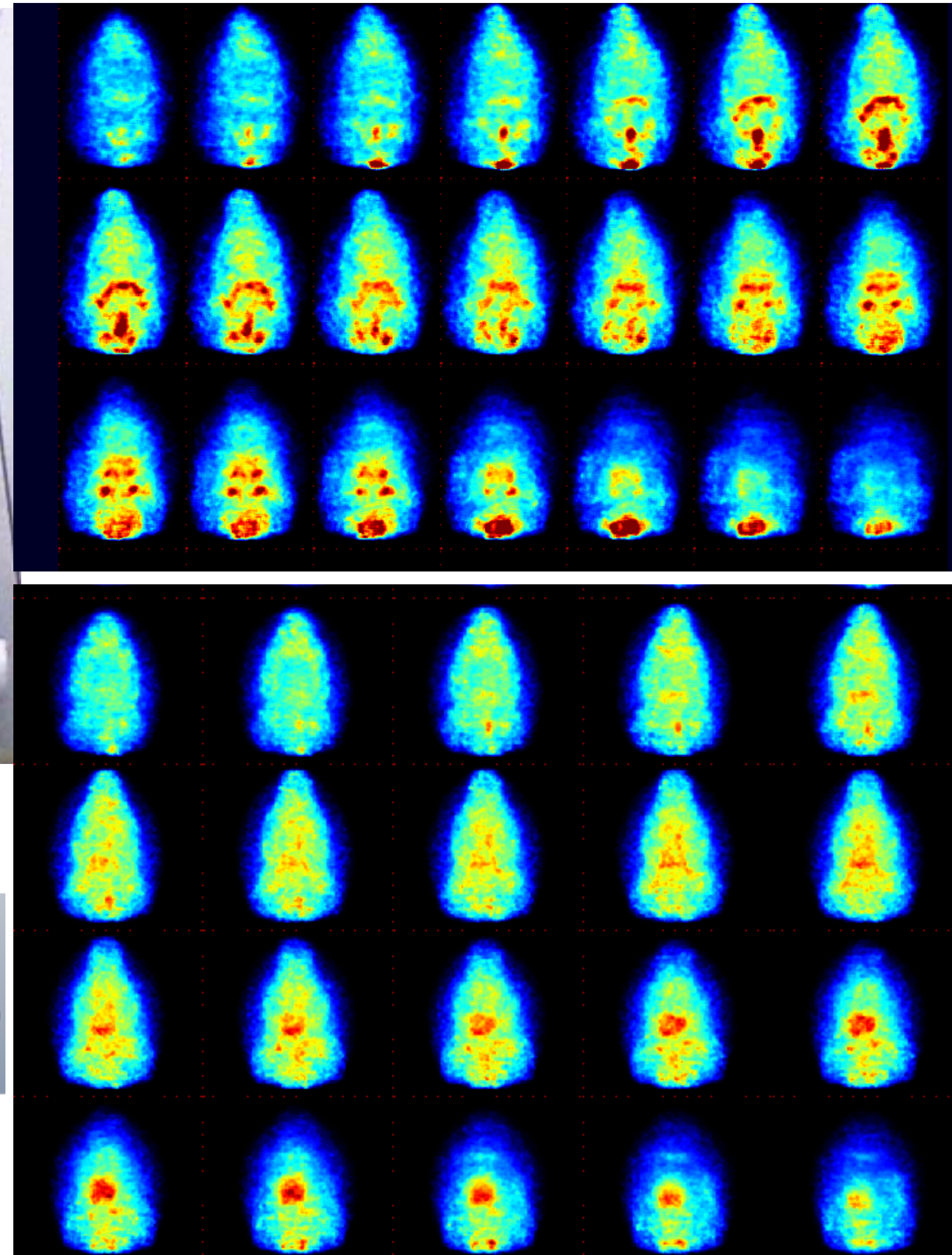

Biology results start to appear

New BACE1 inhibitors decrease Aβ production and accumulation in the 3xtg-AD mouse model [P7/37]

Rosa Resende [1,#], Marisa Ferreira-Marques [1,#], Teresa Dinis [1,2], Francisco Oliveira [3], José Sereno [3], Antero Abrunhosa [3], Miguel Castelo Branco [3,4], Cláudia Pereira [1,5], Armanda E. Santos [1,2]

[1] *Center for Neuroscience and Cell Biology, University of Coimbra, Coimbra, Portugal*
[2] *Faculty of Pharmacy, University of Coimbra, Coimbra, Portugal*
[3] *ICNAS, University of Coimbra, Portugal*
[4] *Institute for Biomedical Imaging and Life Sciences, Faculty of Medicine, University of Coimbra, Portugal*
[5] *Faculty of Medicine, University of Coimbra, Coimbra, Portugal*
[#] *These authors contributed equally to this study*

Congress of the Portuguese Society of Biochemistry, 2016

Several other studies in the pipeline

Expected performance vs. other systems

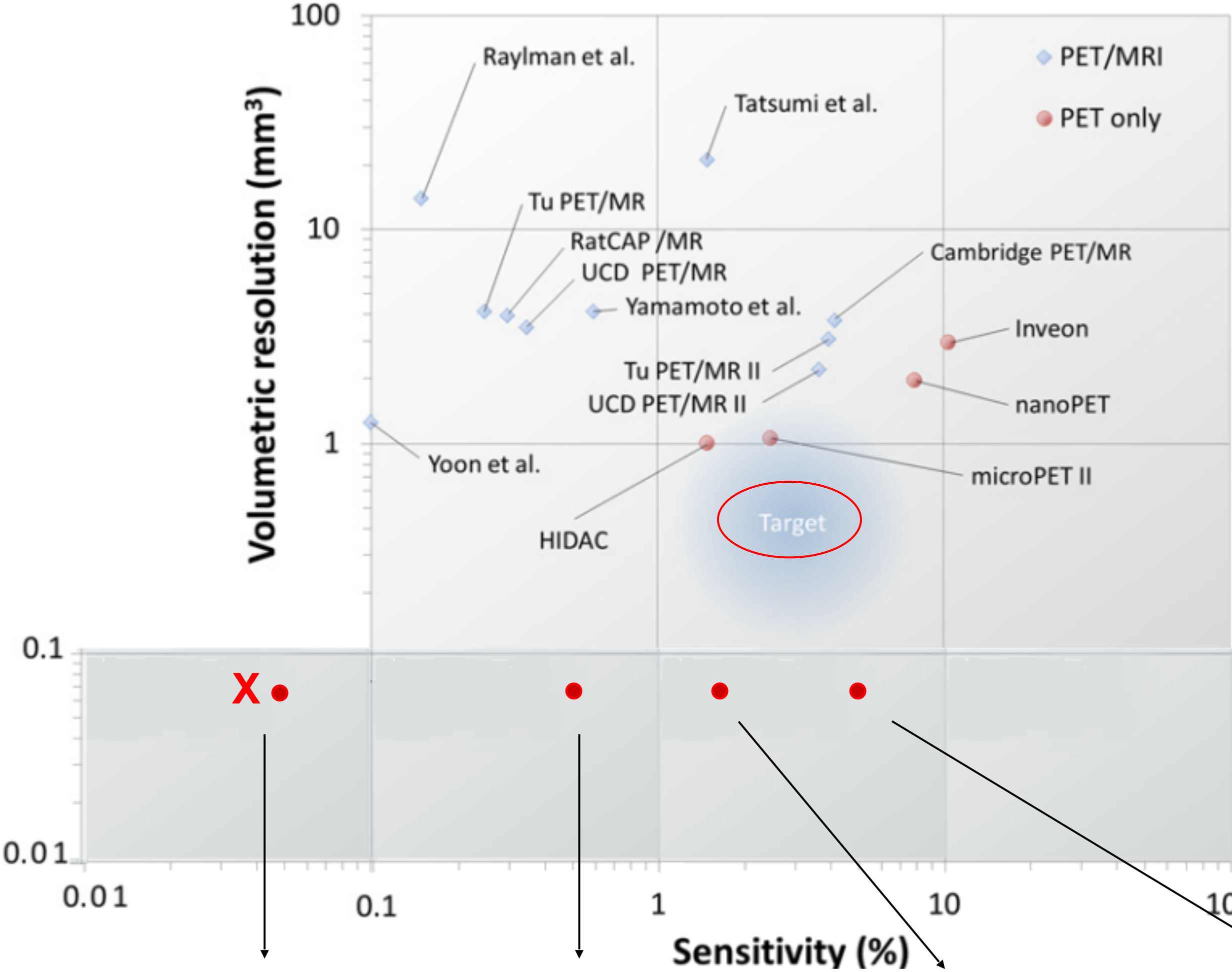

Image adapted from
Applications for Preclinical PET/MRI,
Martin S. Judenhofer and Simon R. Cherry
Semin Nucl Med 43 (2013)19-29

Expected performance exceeds the "target"

X Experimental
● FLUKA simulation

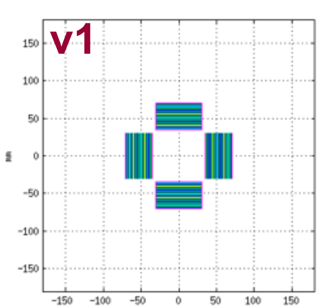

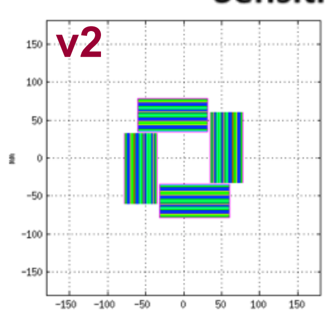

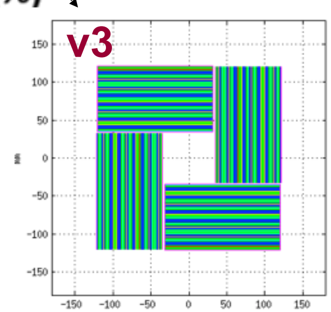

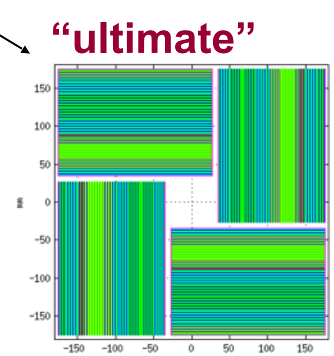

Sensitivity is important… in some cases

Syringe with 70 uCi , 0.5 mm bins

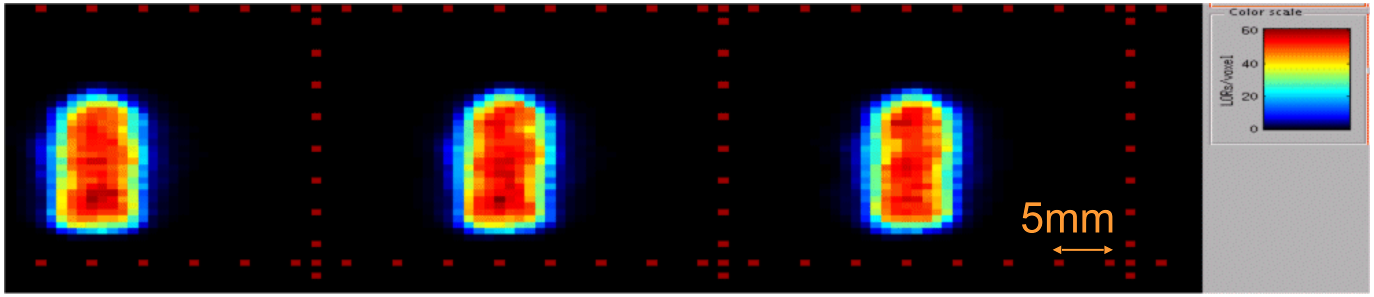

20' in V1
(2' in V2)
60 LORs/voxel
noise ~10%

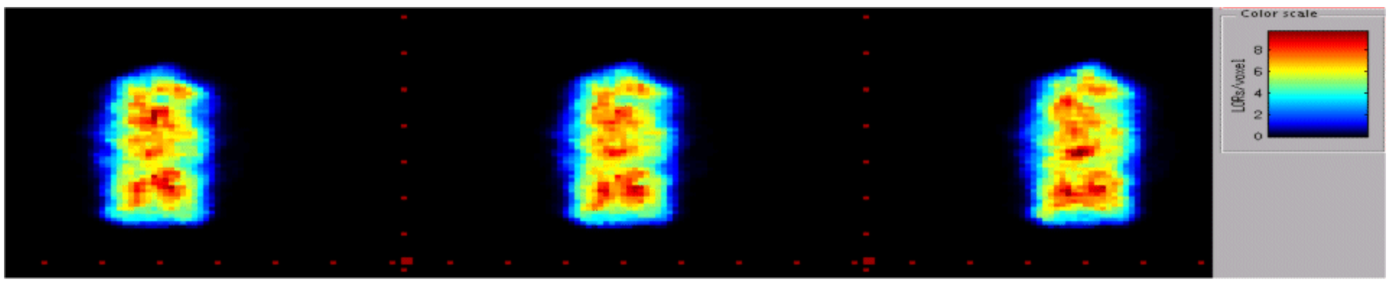

2' in V1
6 LORs/voxel
noise~50%

sub-mm source 10 uCi, 0.2 mm bins, **80s** in V1

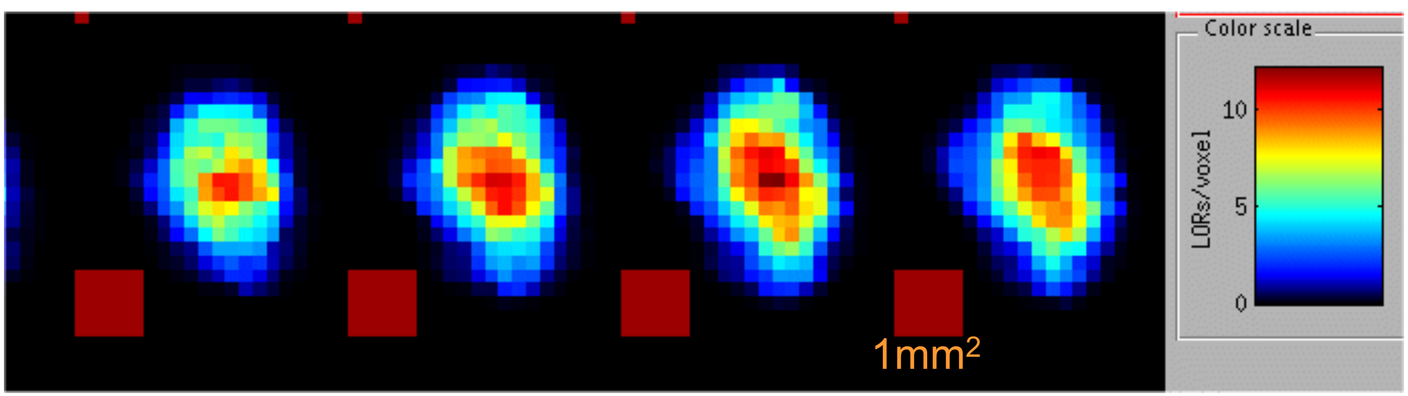

(this is NOT a resolution test)

Full-body human RPC TOF-PET

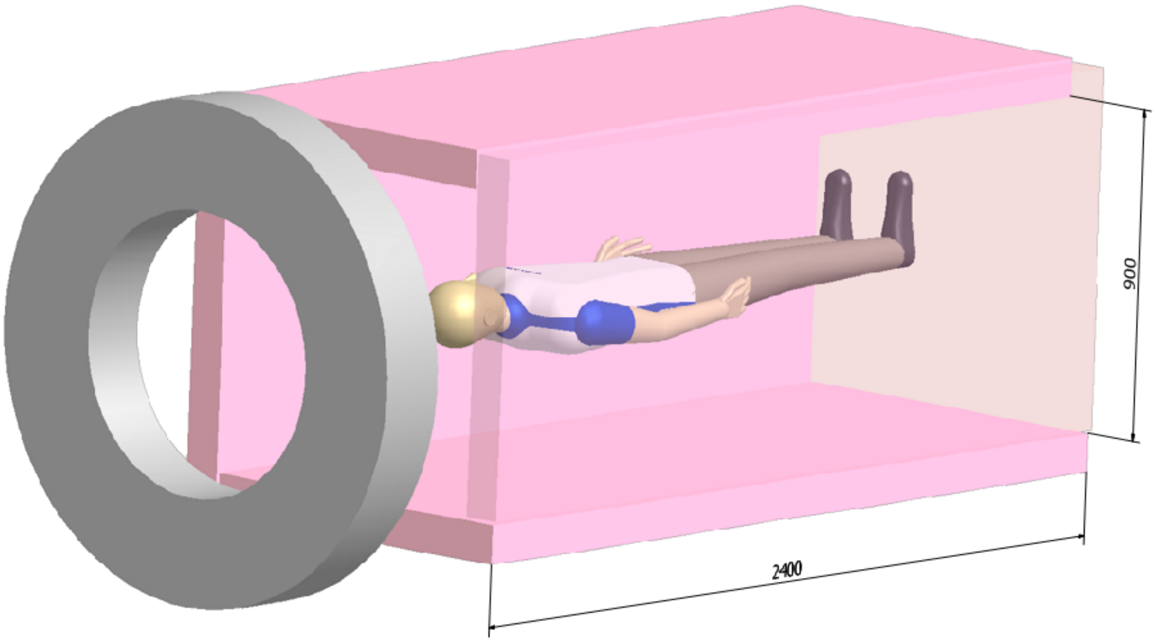

Idea of human RPC-PET

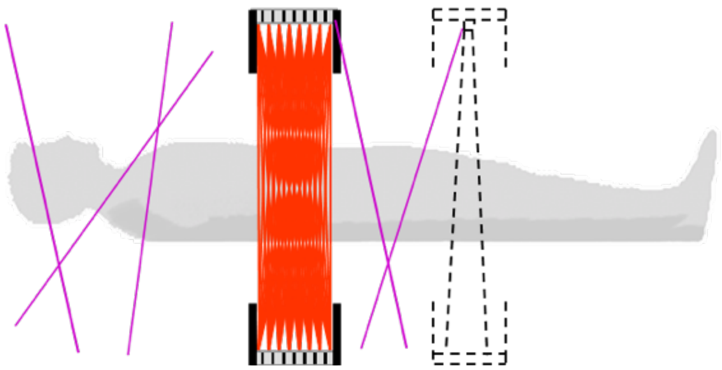

Low geometric efficiency

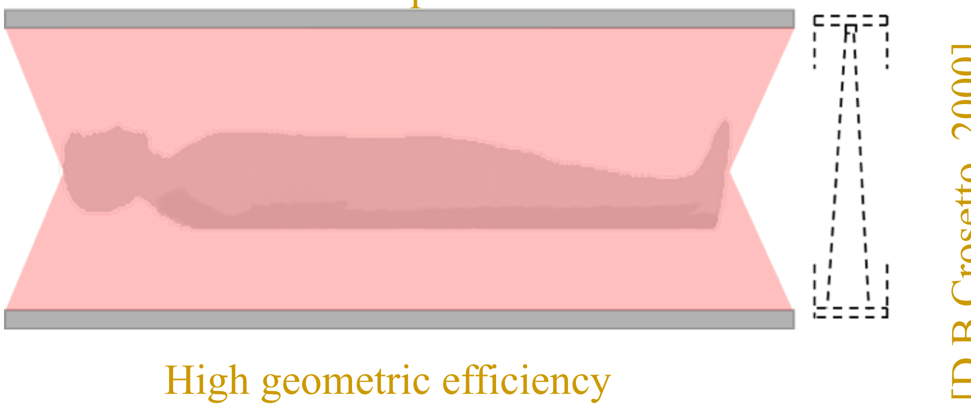

High geometric efficiency

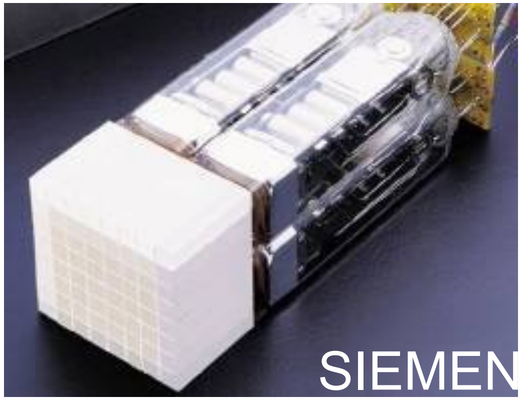

High detection efficiency
Good energy resolution (~ 12% @ 511 keV)
Low time resolution (~ 600 ps)
High cost (cristal + PMTs + electronics)

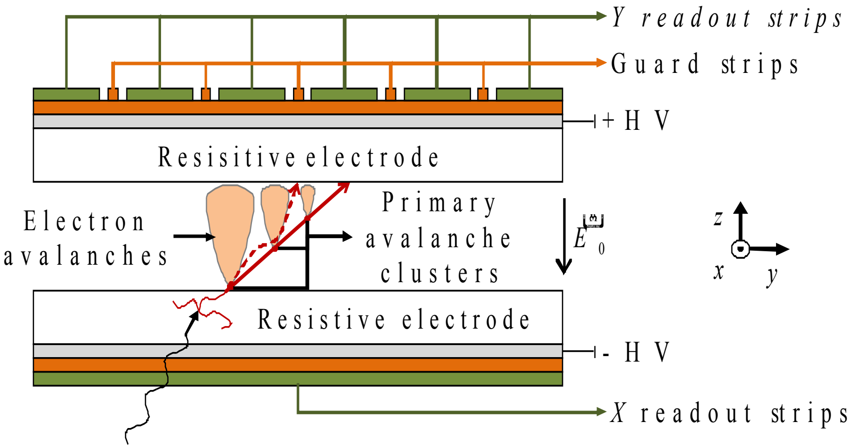

Low detection efficiency (~ 0.2% @ 511 keV)
No energy resolution (but energy sensitivity)
Reasonable time resolution (300 ps)
Low cost (glass + electronics)

The importance of high sensitivity in PET

Image quality $\propto$ counts/pixel

$$\text{counts/pixel} \propto \frac{\text{activity injected in patient} \times \text{measurement time}}{\text{number of pixels}} \times \text{sensitivity}$$

Lower the injected dose
⇒ PET exam can be used on lower risk patients

Higher resolution possible
⇒ Smaller tumours visible

More examinations per unit time
⇒ Lower examination costs
⇒ More people can afford PET exams

Lives saved through earlier cancer detection

RPC TOF-PET – sensitivity advantage

Table 1: Validation of methods against measurements [4].

Events accepted	Ring difference	Sensitivity (NEMA NU 2-1994) Measured (kcps/μCi/ml)	Simulation (kcps/μCi/ml)	Error (%)
Trues	11	1020	1059	3.8
Trues + Scatter	11	1570	1624	3.4
Trues	17	1248	1246	-0.2
Trues + Scatter	17	1920	1928	0.4

(GE advance)

3.1 NEMA-like sensitivities for different scanners

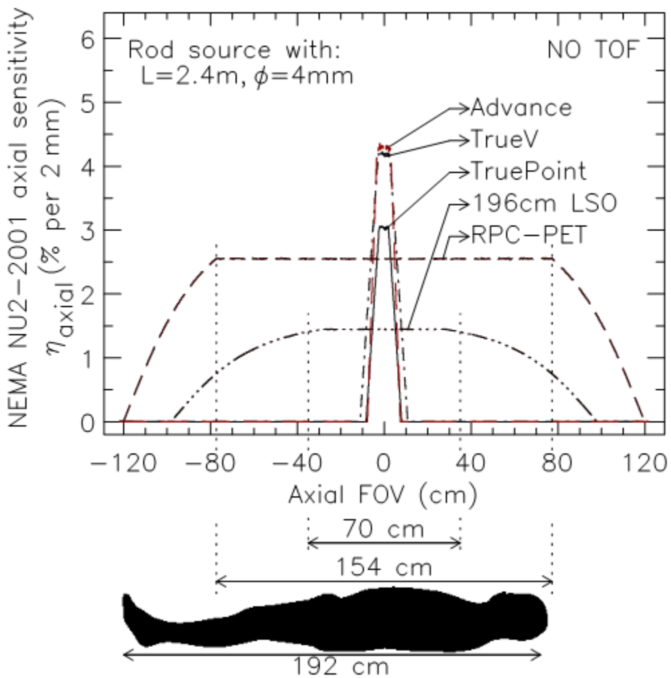

Figure 1: NEMA axial sensitivities for scanners with different AFOV. Details respecting the various PET scanners are given in Table 2. The human figure at the bottom has illustrative purposes only.

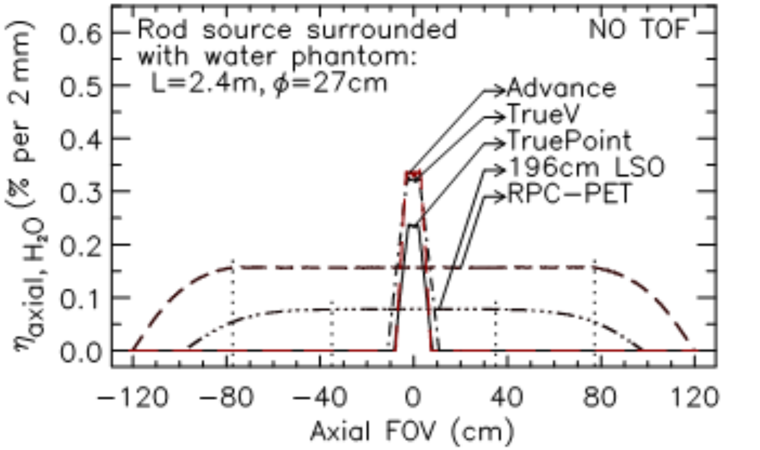

Figure 2: Axial sensitivities similar to Fig. 1, but with the line source immersed in a water cylinder with 27-cm diameter.

3.2 Sensitivity with an athropomorphic phantom

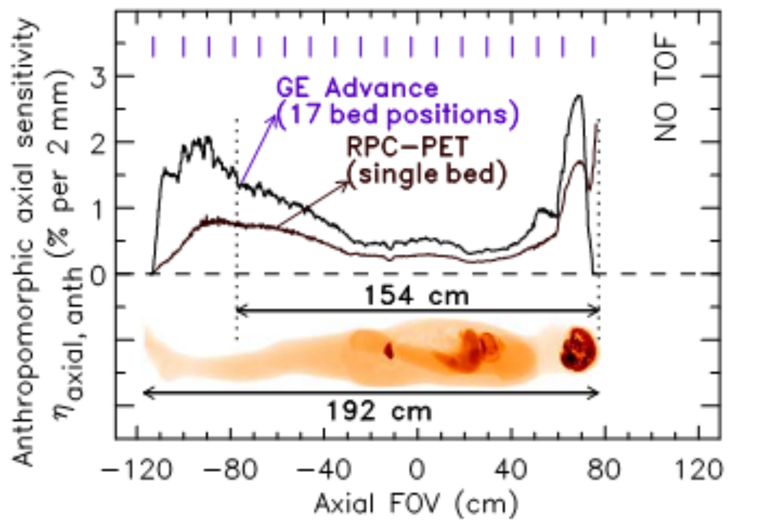

Figure 3: Anthropomorphic axial sensitivities similar to Fig. 2, but simulated with an anthropomorphic phantom adapted to Geant4.

[P.Crespo et al., 2009 IEEE MIC]

RPC TOF-PET – sensitivity advantage

Table 2: Sensitivity performance of several PET scanners simulated with Geant4.

	PET scanner	Biograph[a] TruePoint	Biograph[a] TruePoint TrueV	GE[b] Advance (3D-mode)	196-cm AFOV LSO-based	RPC-PET
	Nb. of block-rings	3[c]	4[c]	3[d]	35[c]	n.a.
	AFOV (cm)	16.2	22	15.2	196	240
	Ring difference	27	38	11	162	$\theta \leq 45°$ [e]
	Packing fraction	0.86	0.86	0.844	0.86	1.0
	Crystal depth (cm)	2.0	2.0	3.0	0.43	n.a.
	Singles efficiency at 511 keV	0.7	0.7	0.78[f]	0.194	0.194
LS in water phantom[i]	Absolute sensitivity, η_a 1.5-m line source (%)	0.013	0.023	0.019	0.066	0.172
	Planar sensitivity[k], η_s (% per 2-mm slice thickness)	0.239	0.327	0.342	0.079	0.158
	Time for equal image quality[l] (min:sec)	2:04 [5]	1:30 [5]	1:27	6:15	3:08
	Scan of 1.5-m length object					
	Nb. of bed steps	14	11	14	1	1
	Total scan time (min:sec)	28:56	16:30	20:18	6:15	3:08
	Relative gain (no TOF)[m]	**1.0**	**1.8**	**1.4**	**4.6**	**9.2**
	Relative gain (with TOF)[m]	**3.0**[o]	**5.4**[o]	n.a.	**13.8**[o]	**55.2**[p]

[P.Crespo et al., 2009 IEEE MIC]

~30-fold sensitivity increase over current state-of-the art scanners

~10-fold if TOF (600 ps) is introduced to LSO scanners

The real benefit of the TOF information is a matter of current research

In here we used the formula:

$$TOF\ sensitivity\ advantage \approx \frac{object\ size}{(c/2)\ time\ resolution}$$

RPC TOF-PET – accepted scatter fraction

anthropomorphic phantom

[P.Crespo et al., 2009 IEEE MIC]

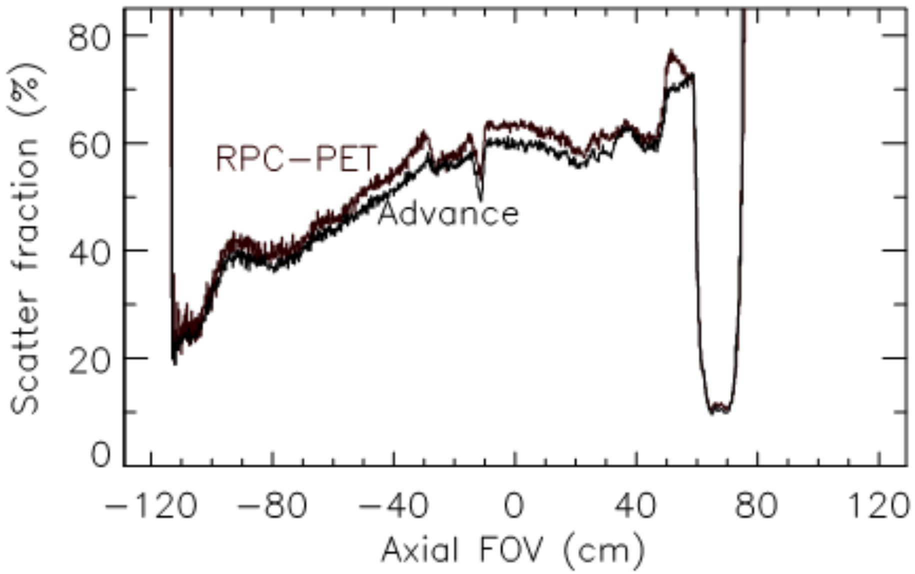

Fig. 6. Axial scatter fraction profiles obtained for the 2.4-m long RPC-PET system, and for a 17-bed scan with the GE Advance.

uniform cylinder phantom

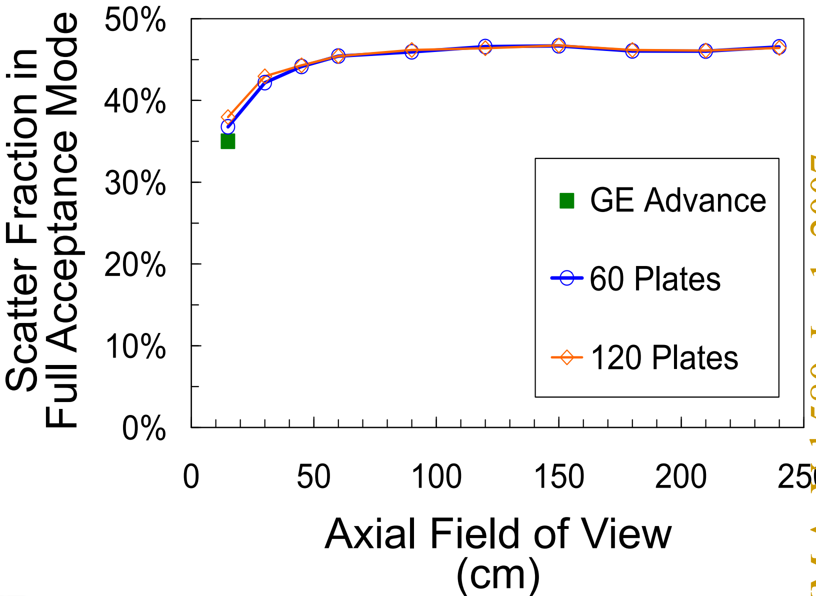

M.Couceiro et al, NIM A, Vol.580, Iss 1, 2007

No apparent handicap for object-scattered photons

Detailed simulations for NECR

M. Couceiro, PhD Thesis, 2014)

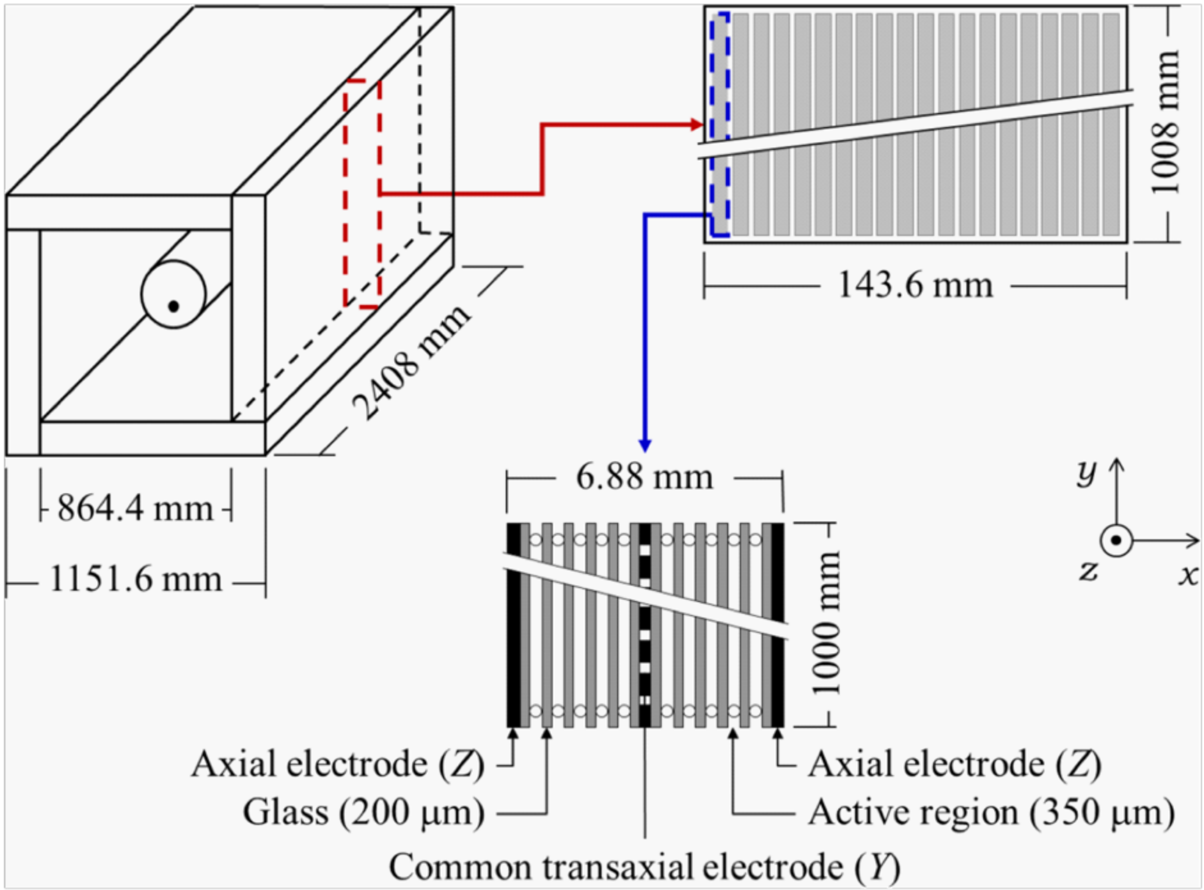

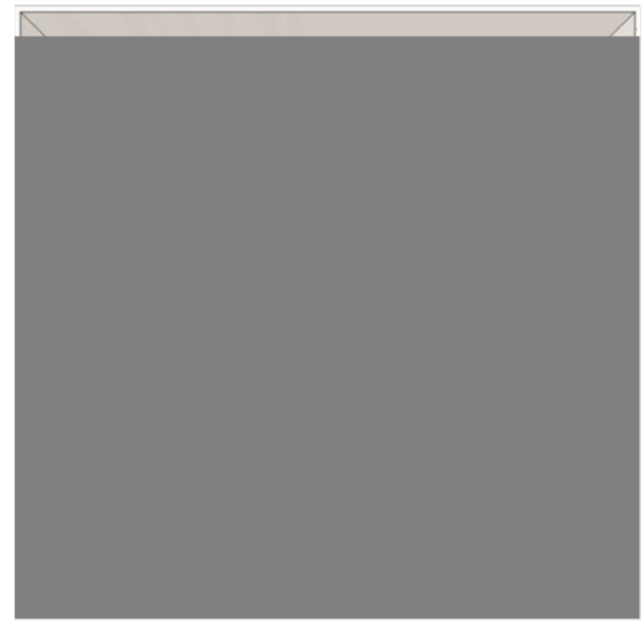

- ✓ The scanner consists in a hollow parallelepiped with 4 detection heads
- ✓ Each detection head has a stack of 20 RPC detectors in the radial direction
- ✓ Each detector consists of 2 RPC modules, each with 5 gaps and independent axial electrodes, but sharing a common transaxial electrode

Detailed simulations for NECR

M. Couceiro, PhD Thesis, 2014)

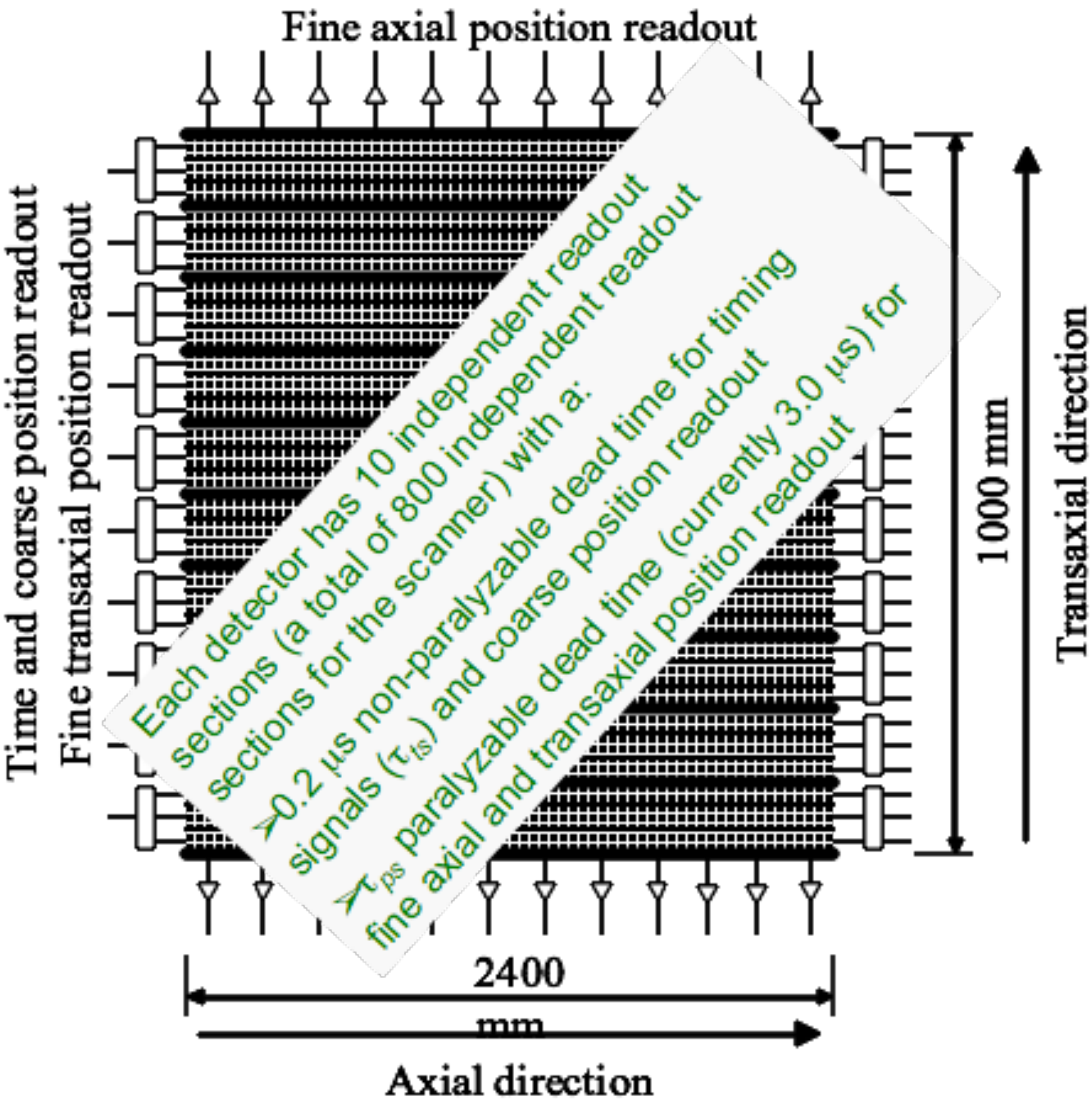

Each detector has 10 independent readout sections (a total of 800 independent readout sections for the scanner) with a:

- 0.2 μs non-paralyzable dead time for timing signals (τ_{ts}) and coarse position readout
- τ_{ps} paralyzable dead time (currently 3.0 μs) for fine axial and transaxial position readout

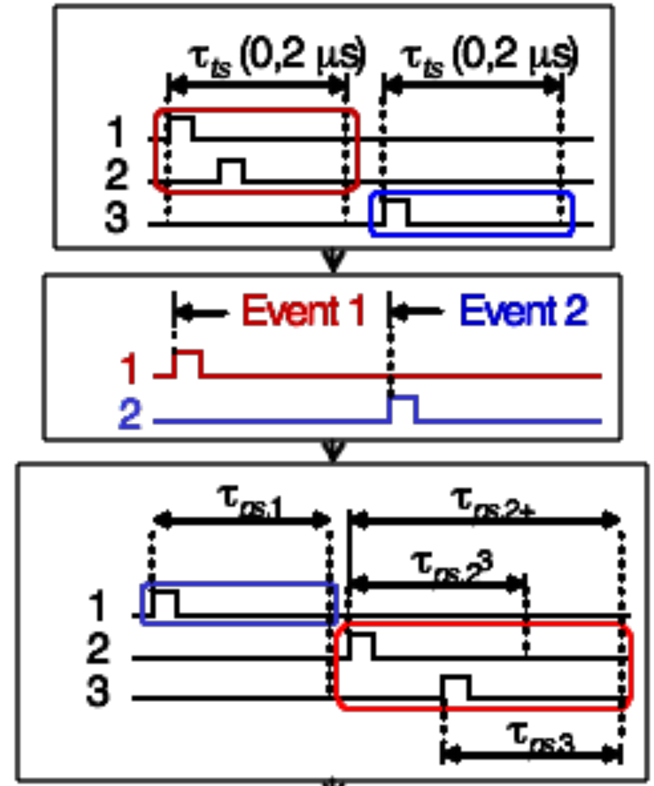

Fine position (3.44 mm pitch in the radial direction and 2 mm pitch in the axial and transaxial directions)

Both events rejected or accepted with coarse position (3.44 mm pitch in the radial direction, 30 mm pitch in the transaxial direction, following a 10 mm σ Gaussian distribution in the axial direction)

Detailed simulations for NECR

M. Couceiro, PhD Thesis, 2014)

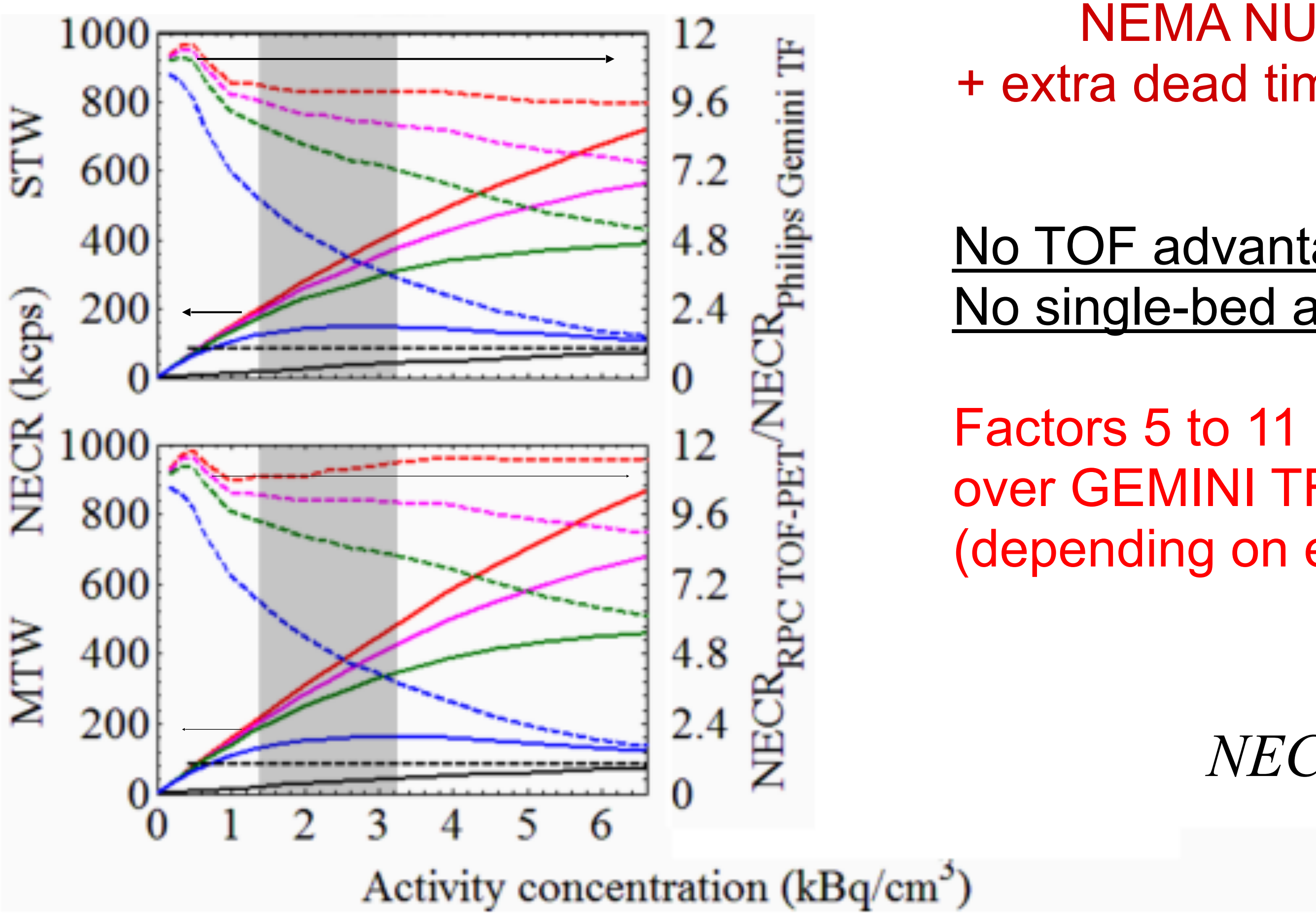

NEMA NU2-2001 - like
+ extra dead time for fine position

No TOF advantage considered
No single-bed advantage

Factors 5 to 11 NECR advantage over GEMINI TF
(depending on electronics dead time)

$$NEC = \frac{T^2}{T + S + 2R}$$

$\tau_{ps} = 0.0\ \mu s$ $\tau_{ps} = 0.5\ \mu s$ $\tau_{ps} = 1.0\ \mu s$ $\tau_{ps} = 3.0\ \mu s$ Solid black line: Gemini TF

$NECR \rightarrow$ left Y axes

$\frac{NECR_{RPC\ TOF-PET}}{NECR_{Phylips\ Gemini\ TF}} \rightarrow$ right Y axes

Prototype of the basic human RPC-PET detector module

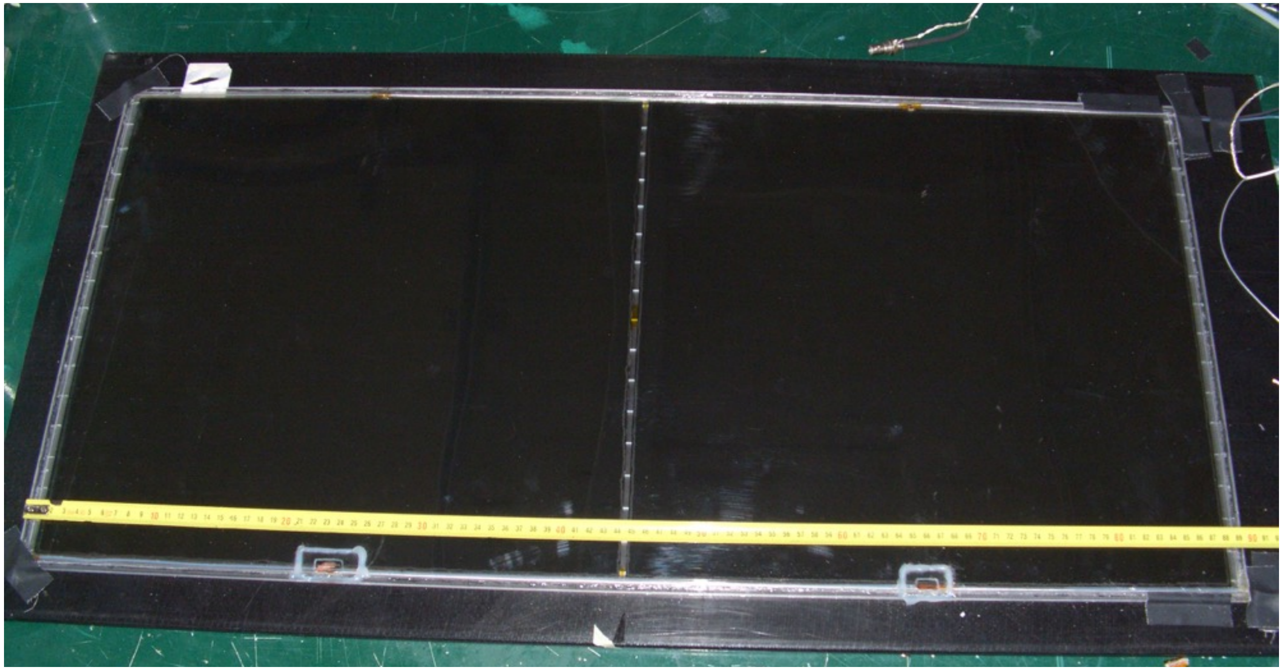

Characteristics:

- 6 glasses of 150±10 μm (a bit too thin)
- 5 gas gaps of 350 μm
- active area 870x415 mm (x6=~2.4m long)
- all high voltage and gas distribution inside

Prototype of human RPC-PET in development

Human PET data chain concept

Multihost support

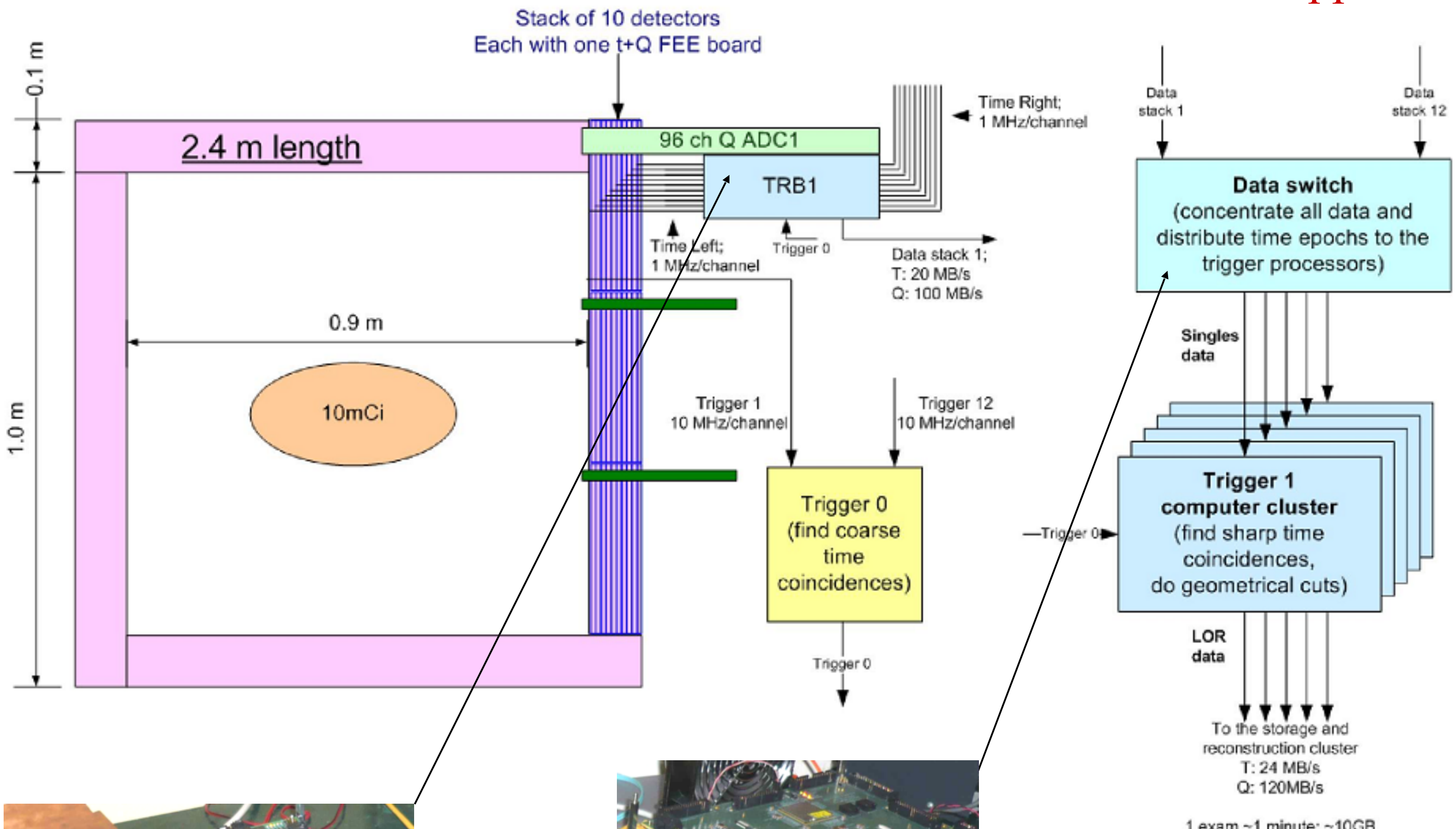

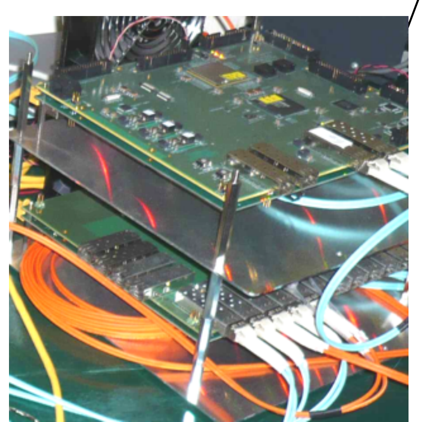

Reconstruction studies - Direct Time-of-Flight Whole Body 3D

NCAT Simulation (whole body)

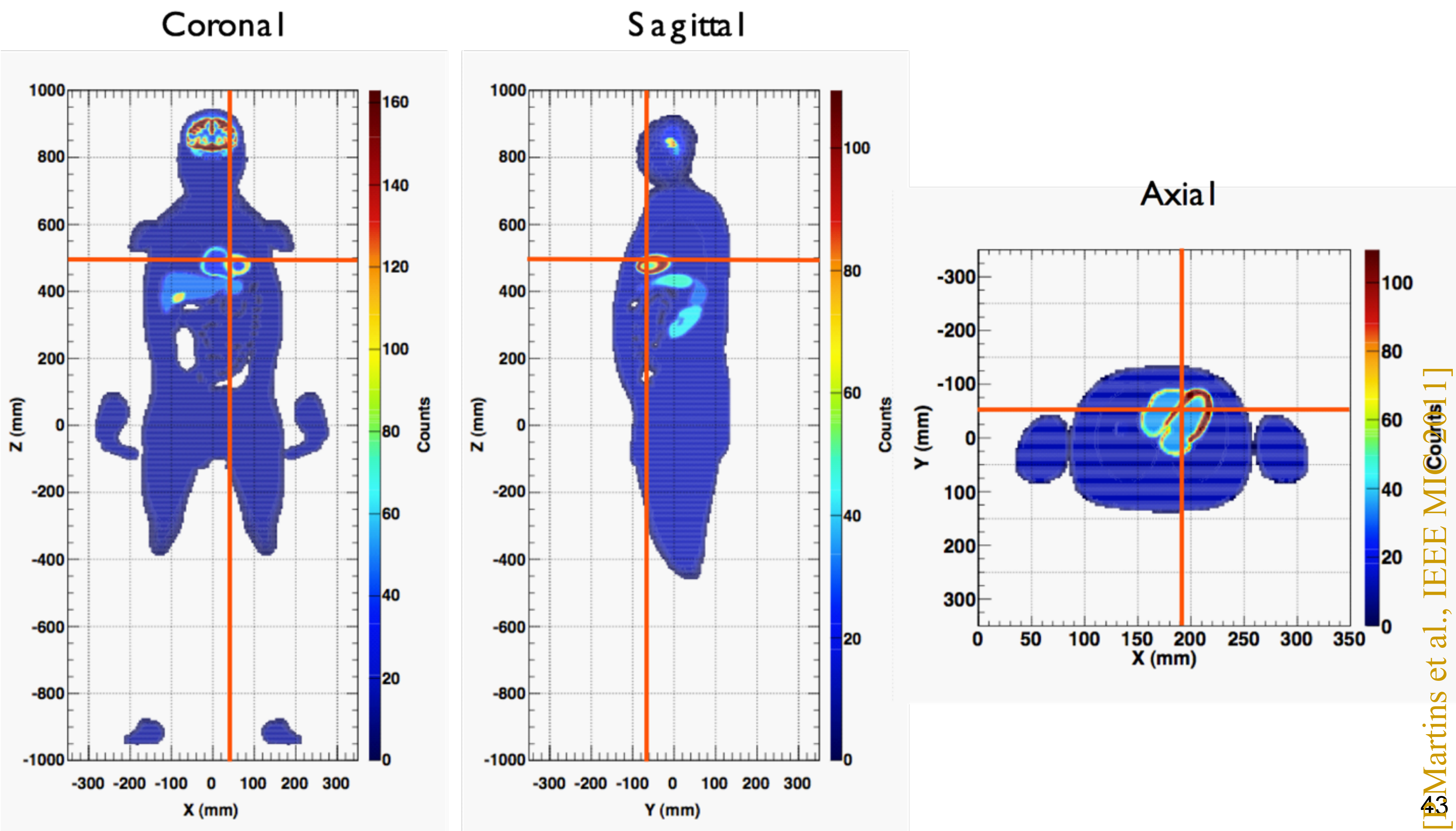

[Martins et al., IEEE MIC 2011]

Reconstruction studies - Direct Time-of-Flight Whole Body 3D

Backprojected Image (300 ps FHWM kernel)

Image quality suggests potential real-time imaging capability of RPC-PET

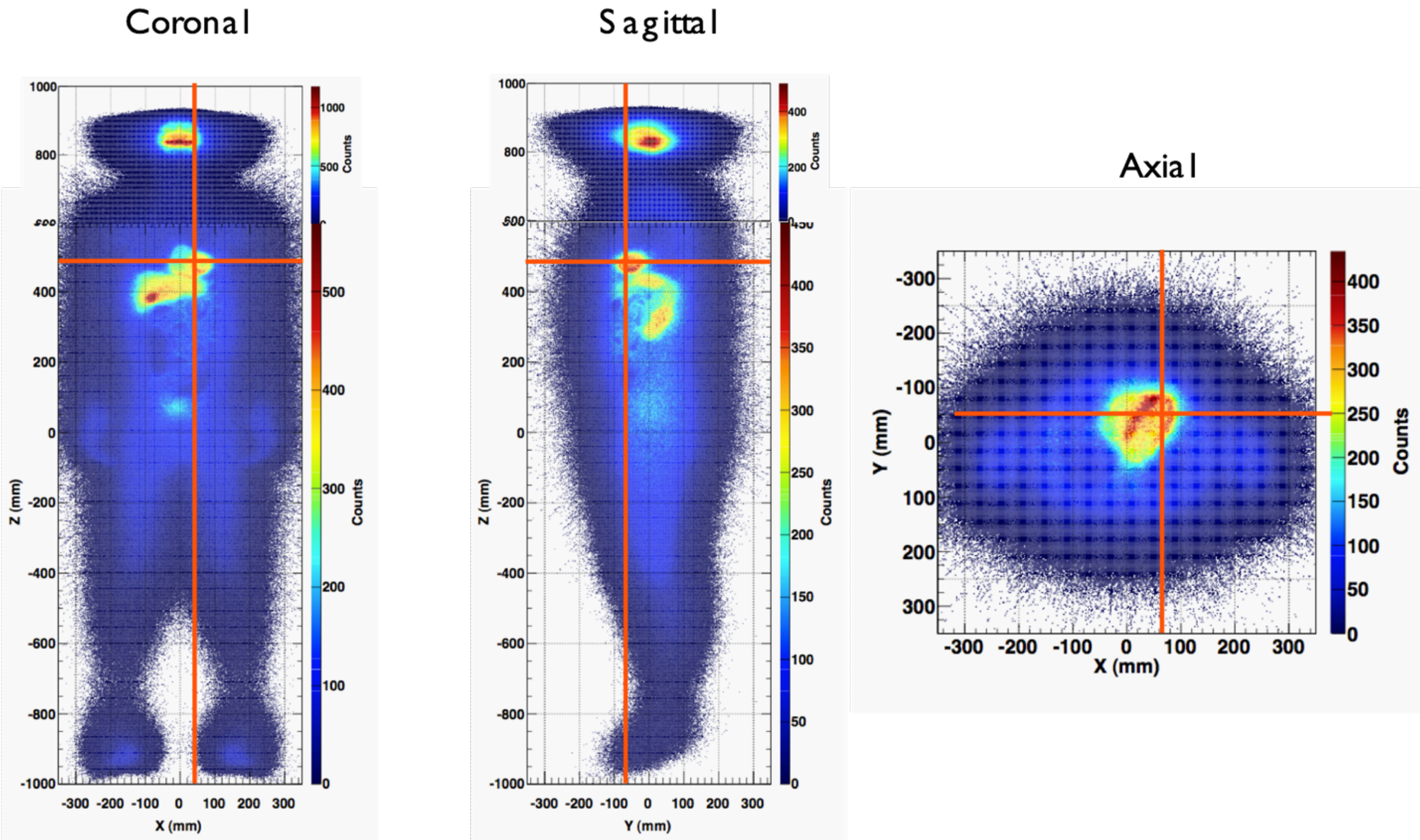

[Martins et al., IEEE MIC 2011]

Reconstruction studies - Direct Time-of-Flight Whole Body 3D

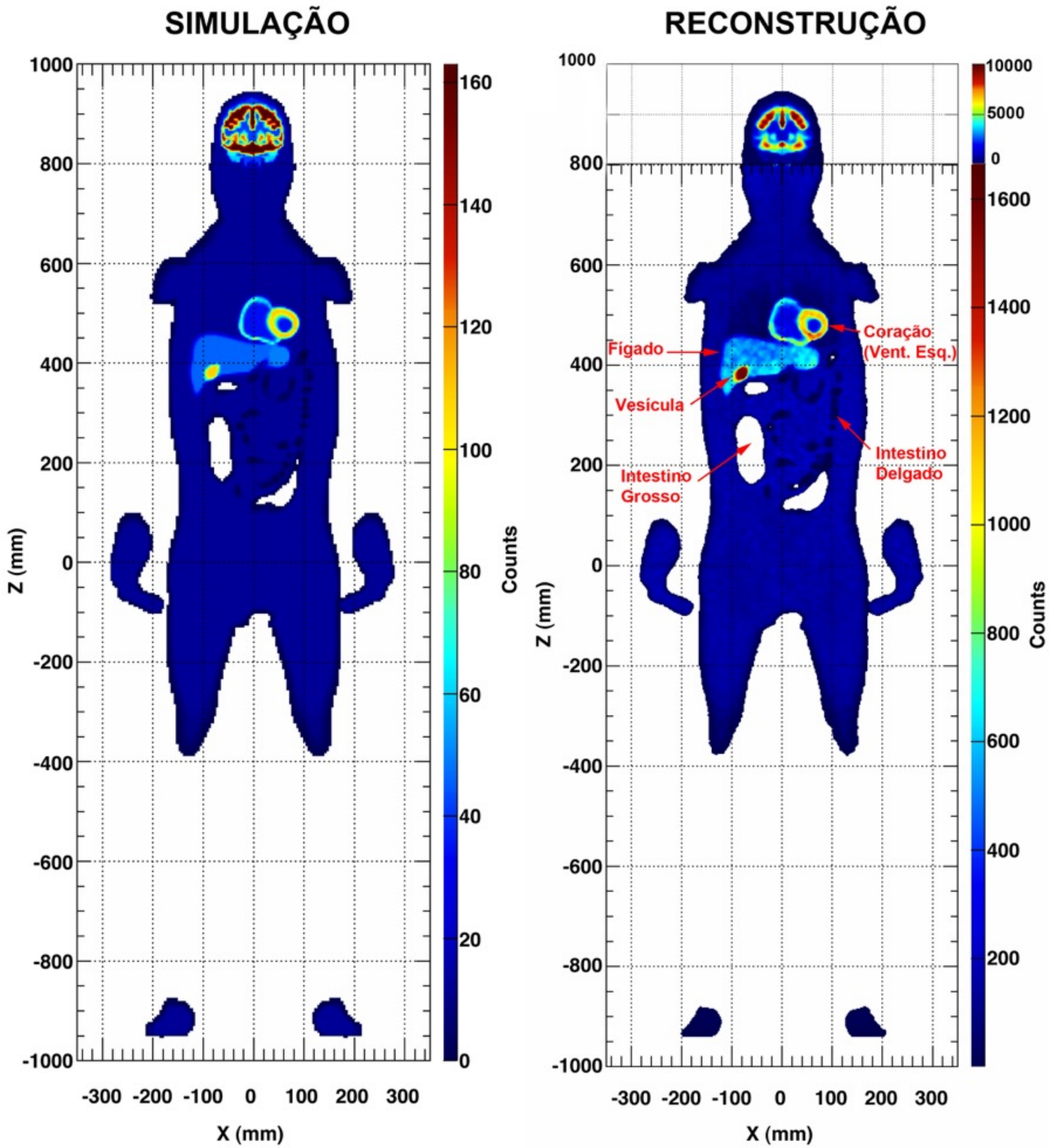

MLEM – 45 iterations

[Martins et al., IEEE MIC 2011]

Reconstruction studies - Direct Time-of-Flight Whole Body 3D

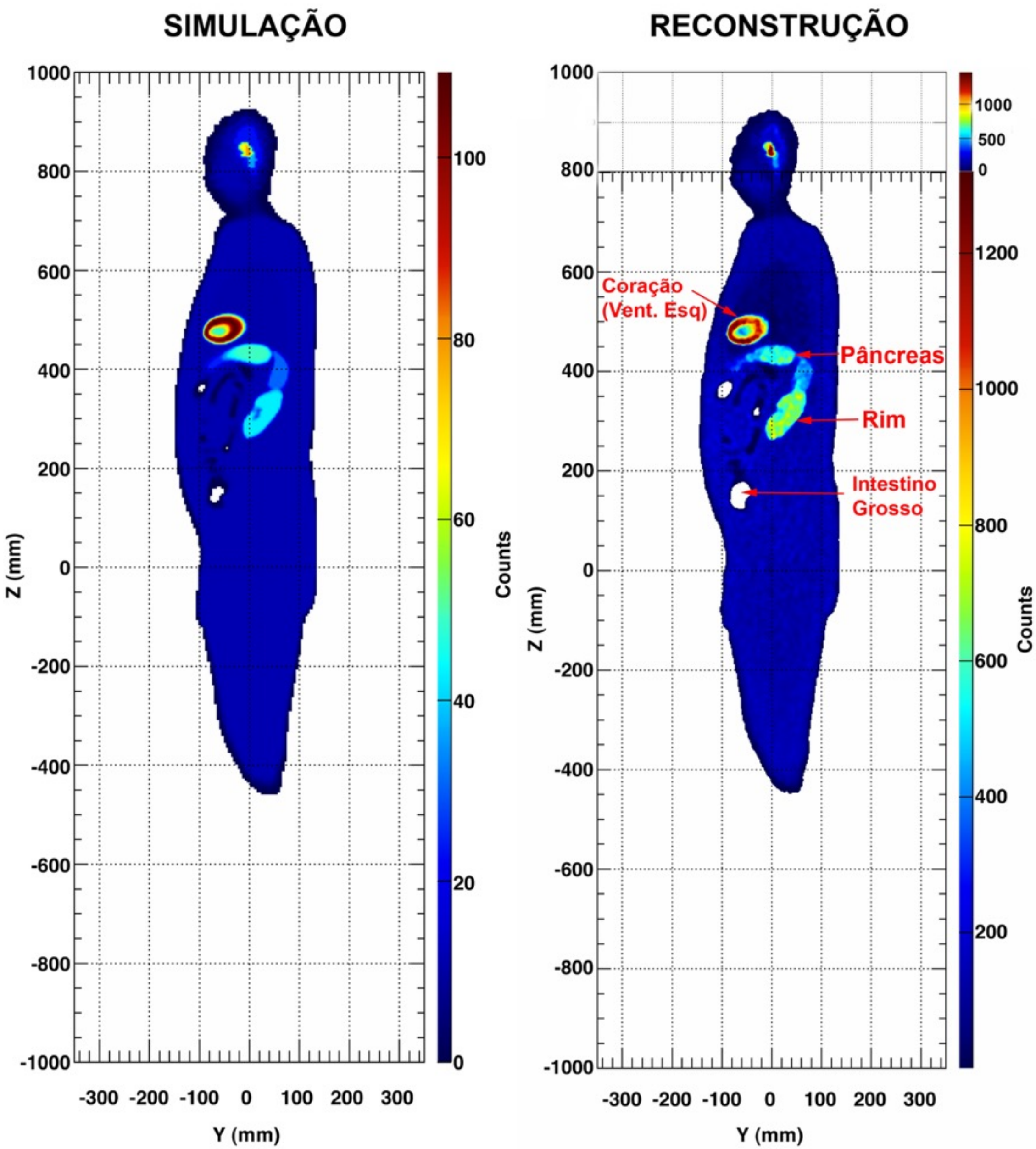

MLEM – 45 iterations

[Martins et al., IEEE MIC 2011]

Reconstruction studies - Direct Time-of-Flight Whole Body 3D

MLEM – 45 iterations

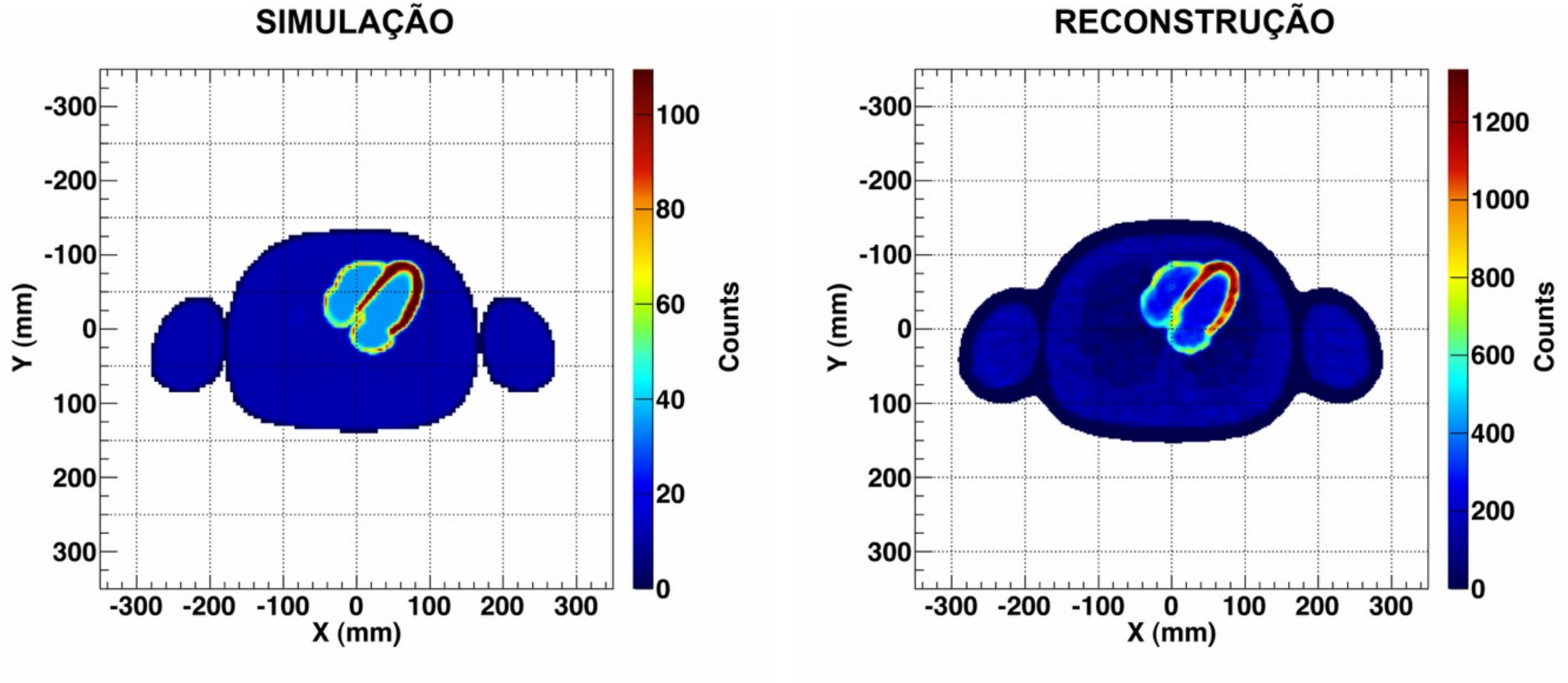

[Martins et al., IEEE MIC 2011]

Summary

Animal RPC-PET

- An excellent space resolution of 0.4 mm FWHM without software enhancements was demonstrated (commercial tomographs >~ 1mm)
- More than 200 mice (and 2 rats) examined so far with ^{11}C, ^{18}F, ^{64}Cu for biological research
- Operated independently by a team at ICNAS
- MRI co-registration via a transfer marker
- V2 in preparation with 10x higher sensitivity and full body FOV for mice
- Simulations and measurements suggest that an extraordinary ultimate performance is possible

Human full body RPC TOF-PET

- Detailed simulations of a human RPC-PET scanner suggest improvements in Noise-equivalent count rate (NECR) up to 11 times over the most sensitive commercial tomograph
- 300 ps FWHM time resolution for photon pairs was demonstrated
- Expected physics-limited resolution (~2mm)
- Funding for a prototype was/is actively procured